MARITIME TRANSPORTATION RESEARCH AND EDUCATION CENTER
TIER 1 UNIVERSITY TRANSPORTATION CENTER
U.S. DEPARTMENT OF TRANSPORTATION

Development of a Design Protocol: Sustainable Stabilization of Slope Using Recycled Plastic Pin in Mississippi

May 01, 2016 to Oct 30, 2017

Prepared by:

Sadik Khan, Ph.D., P.E. (PI)
Assistant Professor
Department of Civil and Environmental Engineering,
Jackson State University,
1400 J. R. Lynch St, Box 17068
Jackson, MS, 39217
Phone: 601-979-6373
Email: J00797693@jsums.edu

Masoud Nobahar
John Ivoke
Graduate Student
Department of Civil and Environmental Engineering,
Jackson State University,
1400 J. R. Lynch St, Box 17068
Jackson, MS, 39217

October 14, 2017

FINAL RESEARCH REPORT

Prepared for:

Maritime Transportation Research and Education Center

University of Arkansas

4190 Bell Engineering Center

Fayetteville, AR 72701

479-575-6021

ACKNOWLEDGEMENT

This material is based upon work supported by the U.S. Department of Transportation under Grant Award Number DTRT13-G-UTC50 to MarTREC. The work was conducted through the Institute for Multimodal Transportation (IMTrans) at Jackson State University (with an U of Arkansas subaward number SA1411041 for JSU), a collaborative proposal with Maritime Transportation Research and Education Center at the University of Arkansas.

DISCLAIMER

Abstract

The maritime and multimodal system is an integral part of the efficient movement of the nation's freight, which includes around 25,000 miles of commercially navigable harbors, channels, and waterways, 4 million miles of public highways and roads, and over 140,000 miles of national, regional, and local railroad networks (Bureau of Transportation Statistics, 2015). Slopes and embankments are one of the major components of the maritime and multimodal transportation infrastructure, which often subjected to shallow landslides due to the existence of expansive clay soil. In Mississippi, the shallow slope failure is induced by the climatic (temperature and rainfall) variation that causes the shrink-swell behavior of expansive Yazoo clay soil and require the significant budget to repair. As a cost-effective alternative, Recycled Plastic Pins (RPP) can be utilized to stabilize shallow slope failures, to offer a sustainable option and increase the economic competitiveness to maintain multimodal transportation infrastructure. The current study investigates the effectiveness of RPP to stabilize shallow slope failure on Yazoo clay in Mississippi, and develops a design protocol, to maintain an efficient, resilient, and sustainable multimodal transportation system. Highly plastic Yazoo clay soil samples are investigated in the laboratory to determine the physical and mechanical soil properties. The laboratory test result is utilized to conduct a safety analysis of unreinforced and RPP reinforced slope using Finite Element Method (FEM) in Plaxis, to evaluate the effectiveness of RPP in Mississippi. The historical rainfall data is assessed in Finite Element Analysis technique over the RPP reinforced slope in coupled flow mode, and associated deformation and safety analysis is conducted to evaluate slope performance under different rainfall condition. Based on the extended FEM analysis results, 3 m long RPPs with the 0.9 m to 1.5 m spacing provide adequate support to stabilize the shallow slope failure in Mississippi.

Table of Contents

List of Figures

List of Tables

Chapter 1: Introduction

1.1 Background

Multimodal transportation systems (MTS) facilitate the efficient movement of people, goods, and services, and are critical national infrastructure components to maintain the nation's economic health. MTS is highly interconnected with numerous other infrastructure systems, which includes communications, emergency response, energy, water supply, agricultural production, and manufacturing. A lack of performance from any one system can have substantial detrimental effects on the performance of the interrelated systems. Slopes and embankments are integral components of the maritime and multimodal transportation system. Shallow failure often causes significant hazards to multimodal transportation infrastructure, and if not properly maintained, it requires more extensive and expensive repairs (Loehr and Bowders, 2007; Loehr et al., 2007). Many of the slopes in the multimodal transportation infrastructure of Mississippi are constructed using marginal highly plastic clay soil (Yazoo clay) which are expansive in nature and are known to be susceptible to shallow landslide. Typically, shallow slope failure occurs due to an increase in pore water pressure and reduction of soil strength due to progressive wetting of soil near-surface soil. This condition is further intensified by moisture variations due to seasonal climatic changes that result in cyclic shrink and swell of the high plastic clay soils. The variation of rainfall, temperature, and soil condition of Mississippi are presented in Figure 1.1, which eventually work as a stressor to cause shallow slope failure.

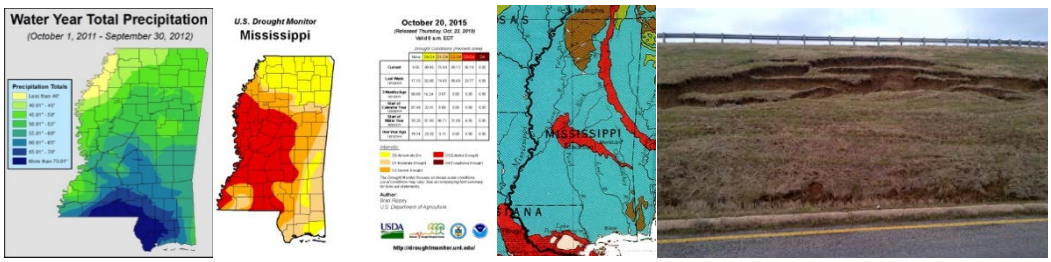

(a) (b) (c) (d)

Figure 1.1 a. Total Precipitation map, b. Drought map, c. Yazoo clay profile in Mississippi, d. Shallow slope failure

The sustainable design of MTS involves the use of low-impact materials, and improve energy efficiency, quality, durability and recyclability principles in design impact measures. Moreover, development of next-generation design concepts for MTS that should include ecological impact, sustainability, and safety impacts of climate and other natural and human-induced hazards in design consideration. A sustainable and cost-effective alternative to stabilize slopes on Yazoo clay in Mississippi can resist the shallow slope failure and lower the maintenance budget, consequently, ensure a sustainable and resilient multimodal infrastructure. The recycled plastic pin (RPP), which is commercially known as recycled plastic lumber (Figure 1.2) is manufactured using post-consumer waste plastic, has been proposed as an acceptable material for use in the construction of docks, piers, and bulkheads. RPPs require no maintenance, is resistant to moisture, corrosion, rot, and insects, and characterized as low impact material on the environment. Several field demonstration projects investigated the effectiveness of RPP to stabilize shallow slope failure over highly plastic clay soil in Missouri, Iowa and Texas (Loehr and Bowders, 2007,

Khan et al. 2013, Khan et al. 2015). The field performance of the stabilized slope indicated that RPP provides resistance against shallow slope failure.

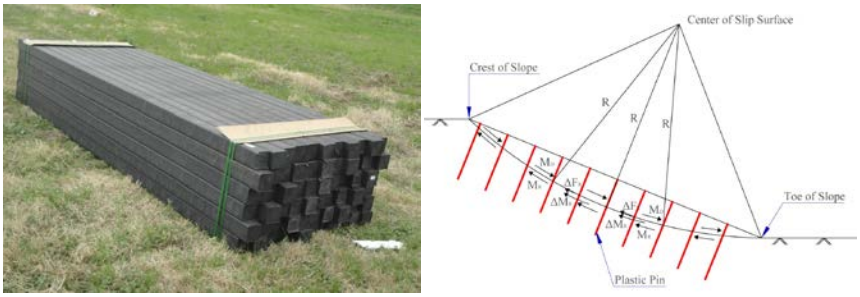

(a) (b)

Figure 1.2 a. A stack of 4" x 4", 10 ft. RPP, b. Schematic of slope stabilization technique using RPP

In Mississippi, the shallow slope failure is induced by the climatic (temperature and rainfall) variation that causes the shrink-swell behavior of expansive Yazoo clay soil and require the significant budget to repair. As a cost-effective alternative, Recycled Plastic Pins (RPP) can be utilized to stabilize shallow slope failures, to offer a sustainable option and increase the economic competitiveness to maintain multimodal transportation infrastructure. The current report summarizes the investigation of the effectiveness of RPP to stabilize shallow slope failure on Yazoo clay in Mississippi.

1.2 Objective of the Study

RPP can be a viable, sustainable, and cost-effective alternative to stabilize the shallow slope failure in Mississippi, because of its significant environmental benefits and cost-effectiveness. The proposed study intends to investigate the effectiveness of RPP to stabilize shallow slope failure in Mississippi, as an alternative to maintain resilient multimodal infrastructure. The specific objective of this research is:

1. To investigate the effectiveness of RPP and
2. Develop a design protocol based on the climatic variation of Mississippi.

High plastic Yazoo clay soil sample from a highway slope will be collected and investigated in the laboratory to determine the physical soil properties. The collected soil samples will also be investigated to determine the peak shear strength; fully soften shear strength and residual shear strength. Moreover, the soil water characteristic curve (SWCC) of the Yazoo clay soil will be developed. A finite element analysis will be conducted with different slope angle to determine the optimum spacing of RPP. Finally, the rainfall pattern of coastal Mississippi will be investigated, and the slope performance under the rainfall will be evaluated.

Chapter 2: Slope Stabilization Techniques

2.1 Stabilization Technique of Shallow slope failure

Different repair methods are used to stabilize surficial slope failures. Selection of an appropriate repair technique depends on several factors, such as the importance of the project (a consequence of failure), budget availability, site access, slope steepness, the availability of construction equipment and experienced contractors. The most commonly used method to repair surficial failures is to rebuild the failed area by pushing the failed soil mass back and re-compact it. Mechanical stabilization techniques utilize rock, gabion baskets, concrete, geosynthetics, and steel pins to reinforce slopes. These techniques can provide stability to both cut and fill slopes (Fay et al., 2012). Mechanical stabilization techniques include retaining walls, mechanically stabilized earth, synthetically reinforced soil and other in-situ reinforcement techniques. For anchoring shallow soils, use of in-situ earth reinforcements and recycled plastic pins has been reported in slope stabilization (Pearlman et al. 1992; Loehr et al. 2000). Earthwork techniques involve the physical movement of soil, rock, and/or vegetation for the purpose of erosion control and slope stabilization. It involves reshaping the surface slope by methods such as creating terraces or benches, flattening over-steepened slopes, soil roughening, or land forming. In addition, earthwork techniques can be used to control surface runoff and erosion and sedimentation during and after construction. (Fay et al., 2012). Different techniques available in practice to stabilize surficial slope failure are presented in the following sections.

2.1.1 Rebuild Slope

Rebuild the slope considers of rebuilding the failed zone through compaction. This method is widespread in Mississippi, which consists of air-drying the failed soil, pushing it back to the failure area, and re- compacting it. Rebuilding the slope is considered one of the most economical methods of repair and is performed as routine maintenance work on failed slopes. However, this method is not effective for most of the scenarios particularly in expansive clays, as the shear strength of soil usually at the residual state, and compaction at the field level does not significantly increase the shear strength, especially when the soil becomes wet again. As a result, repeated slope failures are observed for this method.

2.1.2 Pipe Pile and Wood lagging

This repair method considers installation of pipe pile and wood logging system in the failed zone which provides resistance along the failed soil mass. During the process, the failed debris of the site is disposed of in a different place followed by cutting benches into the natural ground below the slip surface. Galvanized steel pipe piles are then installed (driven or placed in pre-drilled holes) and filled with concrete. Wood lagging (pressure treated) is placed in the piles, and a drainage system is then built behind the wood. A selected fill is compacted in layers, and the face of the slope is protected with erosion control fabric and landscaping (Day, R. W., 1996). The schematic of pipe pile and wood lagging is presented in Figure 2.1.

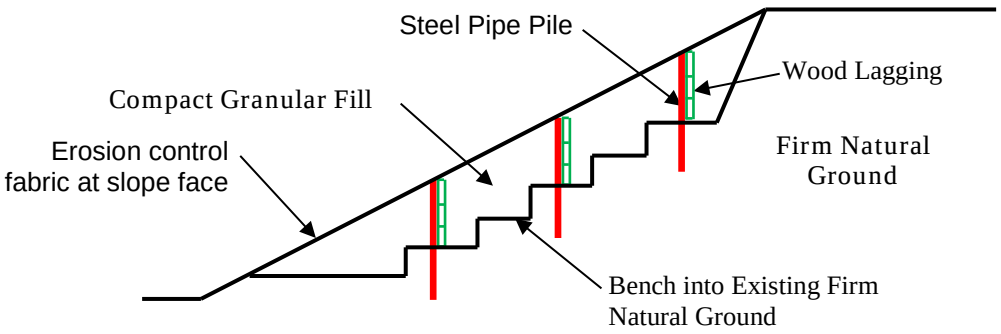

Figure 2.1 Schematic of Pipe pile and wood lagging repair (Day, R. W. 1996)

One of the disadvantages of this method is that lateral soil pressure against the wood lagging is transferred directly to the pipe piles, which are small in diameter and have the low flexural capacity and low resistance to lateral loads. Pile failure in bending is a common occurrence in this repair method (Titi and Helwany, 2007).

2.1.3 **Geosynthetic / Geogrid Repair**

Geosynthetic/Geogrids are fabricated from high-density polyethylene resins and are inserted inside the slopes as soil reinforcement. Reinforced soil slopes (RSS) can generally be steeper than conventional unreinforced slopes as geosynthetics provide tensile reinforcement that allows slopes to be stable at steeper inclinations. According to Elias et al., (2001) the design methods for RSS are conservative so that they are more stable compared to flatter slopes designed to the same safety factor. RSSs offer several advantages over MSE wall. The backfill soil requirements for RSS are usually less restrictive, the structure is more tolerant of differential settlement, and no facing element is required which makes it less expensive compared to MSE wall. Moreover, vegetation can be incorporated into the face of the slope for erosion protection. Geogrid has an open structure which allows interlocking with granular materials used to rebuild slope failures. According to Day, R. W., (1996), repair of surficial slope failures using geogrid materials consists of complete removal of the failed soil mass. Benches are then excavated in the undisturbed soil below the slip surface. Vertical and horizontal drains are installed to collect water from the slope and dispose of it off-site. Finally, the slope is built by constructing layers of geogrid and compacted granular material. The schematic of Geogrid repair is presented in Figure 2.2.

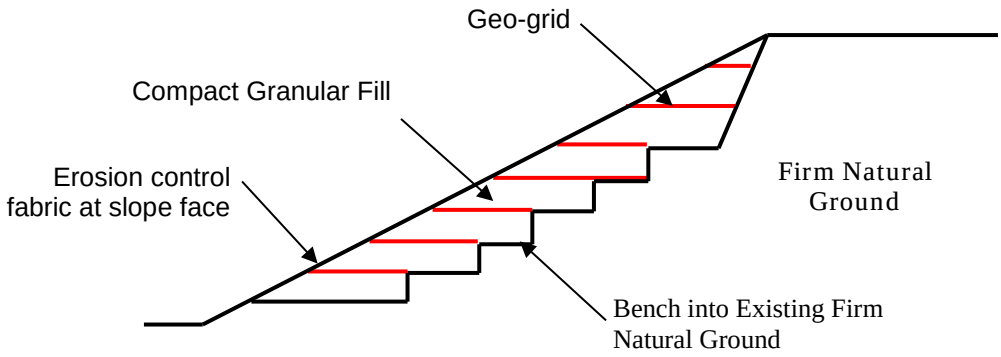

Figure 2.2 Repair of Surficial slope failure by Geogrid (Day, R. W. 1996)

The repair of the slope using geosynthetic/geogrid requires excavating below failure zone, and many require excavation support system during construction, which may drive the repair cost to the very high level.

2.1.4 Soil Cement Repair

The soil-cement repair for shallow slope failure is conducted by excavation and removal of the failed zone similar to the geogrid repair. Benches are then excavated in the undisturbed soil below the slip surface, and drains are installed to collect water from the slope and dispose of it off-site. Granular fill material usually is mixed with cement (~6%), and the mix is compacted to at least 90% of modified Proctor maximum unit weight (Day, R. W. 1996). The soil-cement mix will develop high shear strength and lead to the slope with a higher factor of safety. The schematic of the soil cement repair is presented in Figure 2.3.

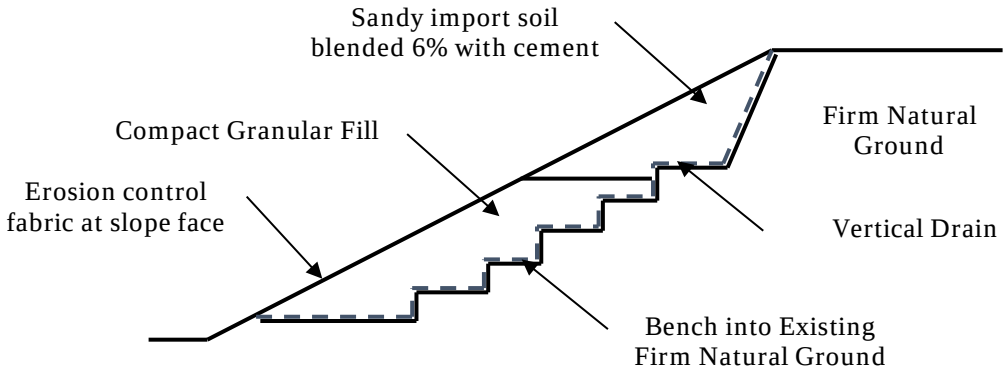

Figure 2.3 Soil cement repair of shallow slope failure (Day, R. W. 1996)

The repair of the slope using this technique may require temporary excavation support system during construction, which may drive the repair cost. In addition, uniformly mixing the cement and treating the clay soil is observed challenging at field condition, which may lead to forming some weak spot in the slope leading to failure.

2.1.5 **Repair using Launched Soil Nails**

Soil nails are inserted into the slope face at high speed utilizing high pressure compressed air. During the technique, the soil nails are installed in a staggered pattern throughout the failed zone which provide resistance along the slipping plane and increase the factor of safety as presented in Figure 2.4. Typical soil nails can be solid or hollow steel bars; however, galvanized soil nails also can be used in highly abrasive environments as they provide resistance to corrosion. Typical hollow non-galvanized steel bars have an outer diameter of 1.5 in. (0.12 in wall thickness) and length of 20 ft., The suggested minimum yield strength of the steel bars is 36 ksi (Titi and Helwany, 2007). After installing launched soil nails, the slope surface can be treated with erosion mat, steel mesh, and shotcrete.

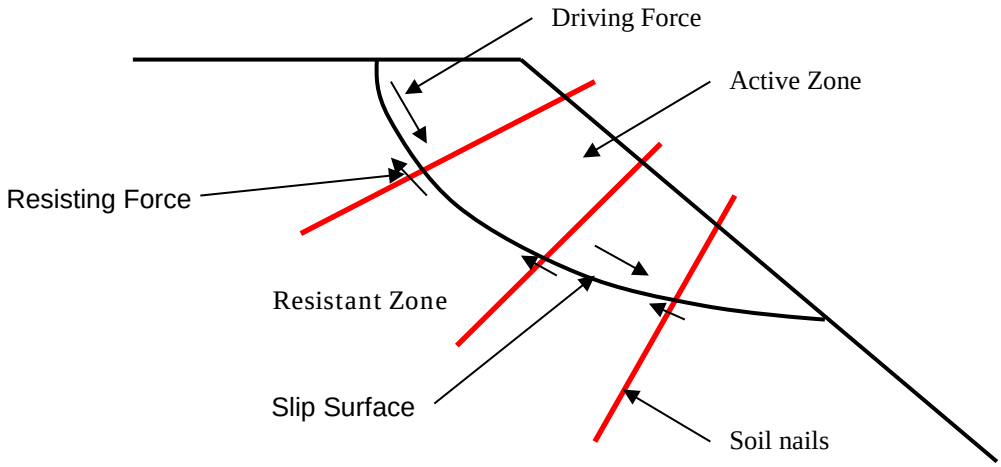

Figure 2.4 Schematic of Repair of soil nails in slope stabilization (replotted after Titi and Helwany, 2007)

Cost of soil nail wall is a function of many factors, including the type of ground, site accessibility, length of the nail, the thickness of facing, type of construction, such as temporary or permanent and availability of skilled manpower. In general soil nail wall are 30% cheaper than tieback wall (Singla, 1999). A major cost item for permanent soil nail wall is the wall facing. In many repairs for slope stabilization in North Texas area, a vertical temporary soil nail wall is constructed to retain the cut section and provide an interrupted flow of traffic. However, these temporary shoring walls contribute a major portion of the total project cost, which also drives high repair cost. Typical cost range for soil nail walls based on U.S. highway project bidding experience ranged between $300/m2 to $600/m2 (Singla, 1999) where the costs are a total in-place cost in dollars per square meter of wall face area.

2.1.6 **Earth Anchors**

Earth anchors have been used in many geotechnical applications including stabilizing surficial slope failures. Earth anchoring systems consist of a mechanical earth anchor, wire rope/rod and end plate with accessories. Repair of surficial slope failures with earth anchoring systems starts with regarding the failed slope. The earth anchors are installed by pushing the anchor into the ground below the failure surface, and wire tendon of the anchor is pulled to move the anchors to its full working position. The wire tendon is locked against the end plastic cap (end-plate) and the system is tightened. A schematic of earth anchors for

stabilizing shallow slope failure is presented in Figure 2.5. The Earth Anchors methods are not successful in fine-grained soil with the presence of water, and its application is limited (Vitton et al., (1998).

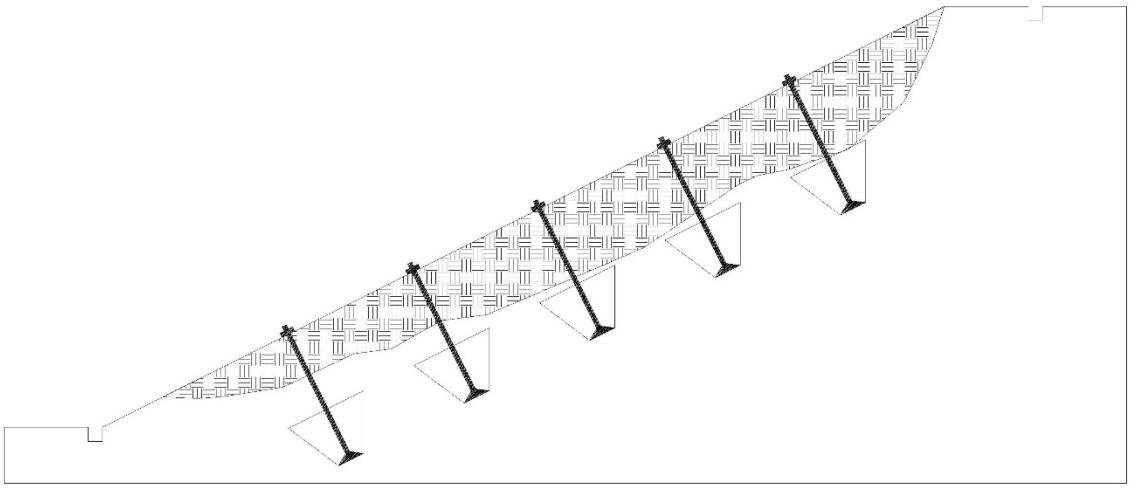

Figure 2.5 Earth Anchors in slope stabilization (redrawn after Titi and Helwany, 2007)

2.1.7 Geofoam

Geofoam is a generic term of rigid cellular polystyrene, is highly used in geotechnical applications and has provided solutions worldwide to many difficult subsoils. The most common type of geofoam is expanded polystyrene (EPS) and extruded polystyrene (XPS). EPS is formed with low-density cellular plastic solids that have been expanded as lightweight, chemically stable, environmentally safe blocks. It generally behaves like elastoplastic strain hardening material. The unit weights of the material ranged from 0.7 to 1.8 pcf and have compression strength ranged between 13 psi to 18 psi. The foam has been utilized to repair problematic highway slopes. During this technique, the failed soil is excavated and the reconstructed using Geofoam. A typical section of the slope repair technique is illustrated in Figure 2.6. The geofoam has considerably low unit weight than soil. However, it has high compressive strength. As a result, the driving force from the soil decrease, which eventually increases the factor of safety of the slope. The field performance result using this technique is promising. Jukofsky et al., 2000 repaired a highway slope in New York using Geofoam. Based on the performance monitoring results, no post-construction lateral movement had taken place. In addition, the extensometer presented negligible movement between the geofoam after construction. Furthermore, the geofoam also works an insulating material and resist the differential temperature variation due to icing. One demerit of this technique is that it requires replacing the failed soil, which may require temporary soil retaining system for construction and repair of the failed slope. As a result, this method may cost prohibitive.

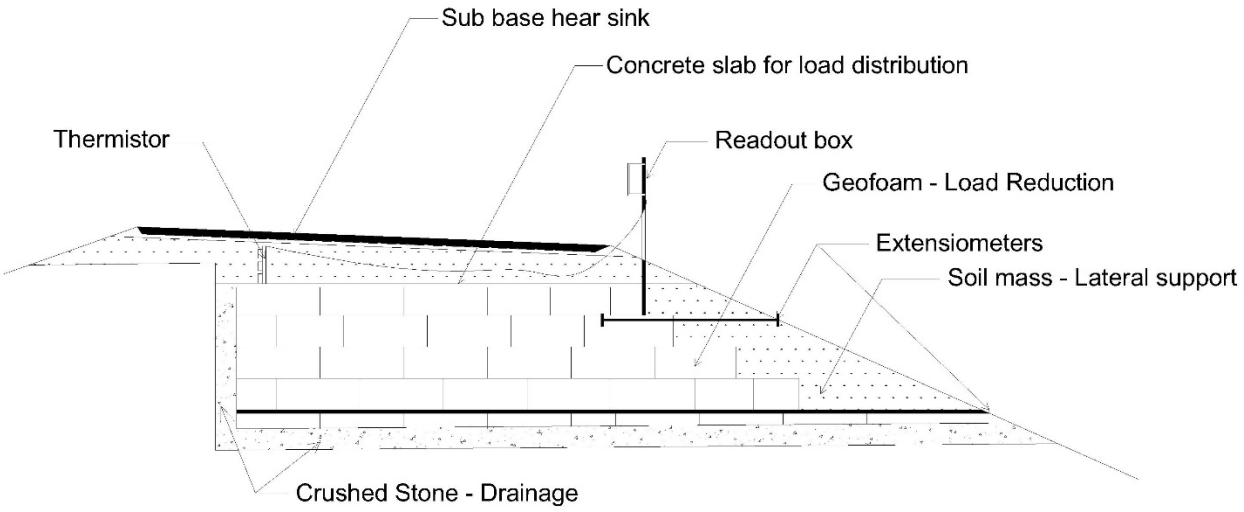

Figure 2.6 Typical section of treatment

2.1.8 **Wick Drains**

Santi, et al. (2001) evaluated horizontal geosynthetic wick drains with a new installation method to determine an effective option to stabilize landslides by reducing amount of water that it contains. Horizontal wick drains are inexpensive; resist clogging and may be deformed without rupture thereby offers several advantages over conventional horizontal drains. A study was conducted by the Santi, et al. (2001) where 100 drains were installed at eight sites in Missouri, Colorado and Indiana using bulldozers, backhoes and standard wick drain driving cranes. The study indicated that drains have been driven 30 m through soil with standard penetration test values as high as 28. In addition, both experience and research suggest that drains should be installed in clusters that fan outward, aiming for average spacing of 8 m for typical clayey soils. Santi, et al. (2001) installed and tested the effectiveness of horizontal wick drains during 1998 in an instrumented embankment in Rolla, Missouri. The embankment which had the slope ratio 1:1 was instrumented with 6 piezometers, 16 nested soil moisture gauge sand 20 survey markers. One half of the slope was stabilized using six wick drains, whether, other half of the slope was kept as control section. The influence of the wick drain was tested by artificial simulation of 100 year, 24-hour rainfall using sprinkler. The result indicated that the wick drain removed substantial amount of water from the slope, thereby lowering the groundwater level by 0.3 m resulted significant less movement in the stabilized zone. Following to the test sites, the author stabilized several locations with varying geology using various driving equipment. No evidence of clogging by dirt or algae was observed after installation and the stabilization scheme was performing better. Based on the experience, Santi et al. (2001) suggested that the drains should not extend more than 3 to 5 m beyond the existing or potential failure surface. In addition, the drains should be installed horizontally, in clusters that fan outward within 8 m spacing. During installation, the smear zone was created that reduce the flow of water. The smear zone could be reduced by pushing pipe that containing the drain, instead of using pounding or vibration method. However, the wick drains have few limitations. For the successful use of wick drains to be driven, the recommended SPT value is 20 or less. The maximum drain length is expected to be 100 ft. for harder soils and 150 to 200 ft. for soft soils. In addition, there could be a significant number of dry drains on a project.

2.1.9 Retaining Wall

Retaining structures are used to retain materials at a steep angle and are very useful when space (or right-of-way) is limited. Low height retaining structures at the toe of a slope makes it possible to grade the slope back to a more stable angle (flat slope) and can be successfully revegetated without loss of land at the crest. Such structures can also protect the toe against scour and prevent undermining of the cut slope. The advantage of using short structures at the top of a fill slope is that it can provide a more stable road bench or extra width to accommodate a road shoulder. Retaining structures can be built external to the slope (such as concrete or masonry retaining wall), or utilize reinforced soil (such as a burrito wall or deep patch) (Fay et al., 2012). It should be noted that using retaining walls in slope stabilization can also apply to large failures such as deep-seated failures; however, this book is primarily focused on stabilizing shallow slope failure. Therefore, examples of low height retaining wall systems are presented in the following sections.

2.1.10 Low Masonry or Concrete Walls

Masonry or concrete retaining walls are rigid structures that do not tolerate differential settlement or movement and are appropriate only at sites where little additional movement is expected. Generally, gravity walls can be constructed with plain concrete, stone masonry, or concrete with reinforcing bar. Masonry walls that incorporate mortar and stone are easier to construct and stronger than dry stone masonry walls; however, they do not drain as well (Fay et al., 2012). Cantilever walls use reinforced concrete and have a stem connected to a base slab. A schematic of a low cantilever retaining wall used to flatten a slope and establish vegetation is illustrated in Figure 2.7. Retaining walls with free-draining compacted backfill can be designed and constructed more efficiently compared to cohesive backfill soils. In this case, a drainage system should be installed behind the wall to facilitate the flow of water in order to resist the formation of perched water zone behind the wall (Fay et al., 2012). The low height retaining wall has been proven to be an effective and well-accepted method in the industry. However, the stabilization using the shallow slope failure by the low height retaining system is cost prohibitive is some case. Moreover, in the fine-grained soil, especially in problematic expansive soil, failure of the wall is common due to lack of sliding resistance. In addition, use of fine-grained soil as a backfill create perched water zone which also increases the lateral pressure on the slope, at the limited performance of the drainage system. A photo of the cracked retaining wall over highway loop 12 in Dallas, Texas, is presented in Figure 2.8.

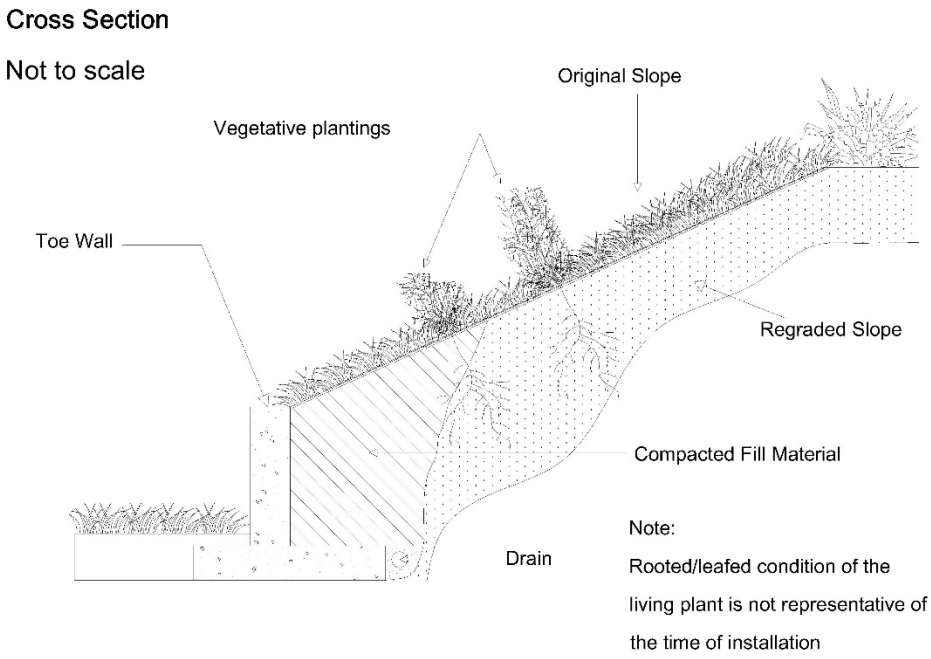

Figure 2.7 Cross section of a low wall with vegetation planted on the slope for stabilization (USDA, 1992)

Figure 2.8 Failure of a low wall over highway loop 12, in Dallas, Texas due to sliding movement

2.1.11 Gabion Walls

Gabion baskets are made of heavy wire mesh and assembled on site, set in place, then filled with rocks. Once the rocks have been placed inside the gabion basket, horizontal and vertical wire support ties are used to achieve the reported strength. Gabion walls are composed of stacked gabion baskets and are considered unbound structures. Their strength comes from the mechanical interlock between the stones or rocks (Fay et al., 2012). Gabion walls can be used at the toe of a cut slope or the top of a fill slope. The walls can be vertical or stepped and are adaptable to a wide range of slope geometries. Gabion walls can

accommodate settlement without rupture and provide free drainage through the wall (Kandaris, P. M., 2007).

2.1.12 **Shallow Mechanically Stabilized Earth Walls**

MSE walls are constructed with reinforced soil as presented in Figure 2.9. The reinforcement can be metal strips (galvanized or epoxy-coated steel), welded wire steel grids, or geogrids. MSE walls can be designed and built to accommodate complex geometries and to heights greater than 80 ft. It offers several advantages over gravity and cantilever concrete retaining walls such as simpler and faster construction, less site preparation, lower cost, more tolerance for differential settlement, and reduced right-of-way acquisition (Elias et al. 2001). The economic savings of MSE walls compared with traditional concrete retaining walls are significantly better at heights greater than 10 ft.; however, short MSE walls can also be constructed economically (Fay et al., 2012). For shallow MSE walls, the less expensive option is usually modular block facing, compared to precast concrete or metal sheet (Elias et al. 2001). It is suggested to use good quality backfill materials to facilitate drainage especially for high walls; however, the short walls can be constructed using poorer quality soils (Fay et al. 2012). The MSE system is a popular choice due to its cost-effectiveness. However, in soft clay foundation soil, the wall has less sliding resistance and may have a recurring failure.

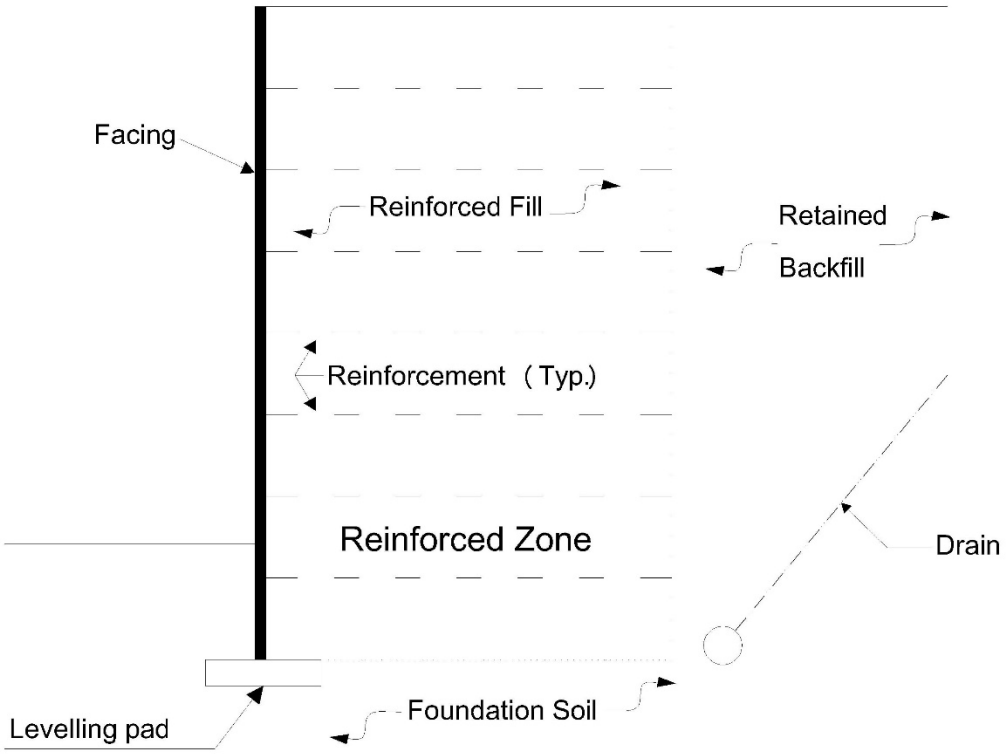

Figure 2.9 Schematic of Shallow MSE wall (Berg et al., 2009)

2.1.13 Pin Piles (Micropiles)

Pin piles (also known as micropiles) are more commonly used for foundations than slope stabilization (Taquinio and Pearlman 1999). The micro pile has great potential to be used for slope stabilization. However, they had been used in insufficient applications. (Fay et al., 2012). The micropiles are primarily used for deep-seated slope failures.

2.1.14 Slender Piles

The flexible and rigid piles are used in slope stabilization application recently. The free field soil movements associated with the slope stability induce lateral load distributions along structural elements which vary with the p-y response, pile stiffness and section capacity of piles. In this case, each pile element offers passive resistance to lateral soil movement by transferring the loads to a stable foundation. Basically, there are two approaches available in the literature known as the pressure based and displacement based method. The stabilizing piles are designed as passive piles in the pressure based method, where ultimate soil pressures are estimated and applied to the piles directly or as an equivalent loading condition. In contrast, the assumptions of the pressure based method are often not satisfied for free headed slender pile elements for cases of larger pile deformation or plastic flow. As an alternative, the pile-soil reaction and passive pile response can be evaluated as a function of relative displacement between the soil and piles. However, evaluation of the relative displacement between the soil and pile is complicated as the pile displacement depends on the soil displacement near the pile; and therefore, the analysis of the displacement response considers the soil-pile interaction.

2.1.15 Plate Piles

Recently, plate piles have been utilized to stabilize shallow slope failure in the state of California. The plate piles increase the resistance to sliding through reducing the shear stress and are installed vertically into the slope similar to the pile-slope system. In a typical application, the plate piles are 6 ft to 6.5 ft long, 2 in by 2 in steel angle iron sections with a 2 ft by 1 ft wide, rectangular steel plate welded to one end (Mccormick and Short, 2006). The plate piles are driven into an existing landslide or potentially unstable slope which have 2-3 ft of soil or degraded clay fill over stiffer bedrock, as presented in Figure 2.10. As a result, the plate reduces the driving forces of the upper slope mass by transferring the load to the stiffer subsurface strata. The critical component in determining initial pile spacing was the angle iron resistance (Short and Collins, 2006). In an experimental test section, the Plate piles were installed in a staggered grid pattern at 4 ft c/c. Depending on the stiffness of the underlying materials, plate pile can be installed either by direct push method by an excavator bucket or driven by either a hoe-ram or “head-shaker” compactor at rates of 20 to 25 blows per hour. This shallow slope stabilization using Plate piles is the latest innovation and presented a lot of potential as an alternative approach. The field implementation and controlled slope experiments conducted by Short and Collins (2006) presented that the plate pile technique can increase the Factor of Safety against slide 20% or greater and can reduce the cost of slope stabilization 6 to 10 times that of convention slope repairs. However, one of the major demerits of the technique included the failure depth that ranged only 3 ft.

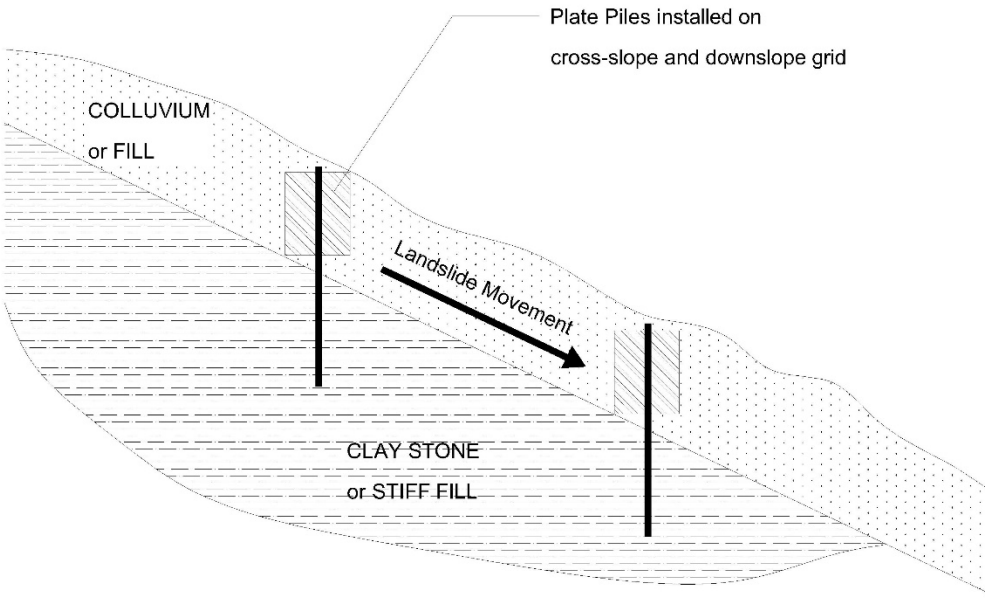

Figure 2.10 Schematic of Plate Pile for Slope Stabilization (Short and Collins, 2006)

2.2 Recycled Plastic Pin

Recycled Plastic Pins (RPP) has been utilized in the state of Missouri, Iowa and Texas, as a cost-effective solution for slope stabilization compared to conventional techniques (Loehr and Bowders, 2007, Khan et al., 2015). Typically, RPPs are fabricated from recycled plastics and waste materials such as polymers, sawdust and fly ash (Chen et al., 2007). It is a lightweight material and less susceptible to chemical and biological degradation compared to other structural materials. RPPs are installed in the failed area to provide resistance along the slipping plane to increase factor of safety. RPP has significant financial and environmental benefits to stabilize shallow slope failure. The recycled plastic pin, which is commercially known as recycled plastic lumber is manufactured using post-consumer waste plastic has been proposed as an acceptable material for use in the construction of docks, piers, and bulkheads, etc. Plastic lumber is also marketed as one of the environmentally preferable materials. Based on environmental and life-cycle cost analysis (LCCA) standpoint, the recycled plastic pin (RPP) is under serious consideration as structural materials for marine and waterfront application. The RPP require no maintenance, is resistant to moisture, corrosion, rot, and insects. It is made of recycled, post-consumer materials and helps to reduce the problem associated with disposal of plastics. Typically, 50% or more of the feedstock used for plastic lumber composed of polyolefin in terms of high-density polyethylene (HDPE), low-density polyethylene (LDPE) and polypropylene (PP). The polyolefin acts as adhesive and combines high melt plastics and additives such as fiberglass, wood fibers within a rigid structure. Moreover, additives are added during the manufacturing process of recycled plastic lumber which includes, foaming agents, ultra-violate (UV) stabilizers, and pigments.

2.2.1 Manufacturing Process of RPP

The manufacture of plastic lumber begins with the collection of raw materials. After collection, the plastic is cleaned and pulverized. The resulting confetti arrives at the production site where it is melted in an extrusion machine. Malcolm, G. M. (1995) presented two methods of manufacturing the recycled plastic

lumber, 1. Injection molding process and 2. Continuous extrusion process. In an injection molding process, the molten plastic is injected into a mold that defines the shape and length of the product. The mold is then cooled uniformly, and the product is removed from the mold. The process is relatively simple and inexpensive. However, the production volume is limited (Malcolm, G. M., 1995). The continuous extrusion process allows producing a varying length of the recycled plastic lumber. During this process, the molten plastic is continuously extruded through series of dies which shape the materials during its cooling. However, it is challenging for the manufacturer to provide uniform controlled cooling of the sample to prevent warpage and caving of the lumber. It should be noted that continuous extrusion process requires considerable investment compared to the injected molding process. However, this process requires less labor and is suitable for mass production quickly. Another manufacturing process of the recycled plastics that is widely used is the compression molding process (Lampo and Nosker, 1997). This process mixes batches consisting of 50-70% of thermoplastics with other materials by melting. An automatically adjusted scraper then removes the melted material from the plasticator and presses it through a heated extruder die into premeasured, roll-shaped loaves. The loaves are then conveyed to a press-charging device that fills a sequence of compression molds alternately. The products are cooled in the molds to a temperature of 40°C and ejected into a conveyor which carried it to a storage area.

2.2.2 Engineering Properties of RPP

Bowders et al. (2003) conducted a study on the different engineering properties of RPP. The motivation of the study was to evaluate the engineering properties of wide varieties of production standard and to develop specifications for the slope stabilization. As a part of the study, uniaxial compression tests and four-point flexure test were performed. The samples were collected from three manufacturers. The experimental results for the uniaxial compression and four-point bending test are presented in Table 2.1and Table 2.2, respectively.

Table 2.1 Uniaxial compression test results (Bowders et al., 2003)

Specimen Batch	No. of Specimen tested	Nom. Strain Rate (%/min)	Uniaxial Compressive Strength (MPa)		Young's Modulus, E1% (MPa)		Young's Modulus E5% (MPa)	
			Avg.	Std. Dev.	Avg.	Std. Dev.	Avg.	Std. Dev.
A1	10	-	19	0.9	922	53	390	27
A2	7	0.005	20	0.8	1,285	69	378	15
A3	6	0.006	20	0.9	1,220	108	363	27
A4	3	0.004	20	0.9	1,377	165	363	25
A5	4	0.006	12	1	645	159	225	17
A6	4	0.006	13	0.9	786	106	238	34

Specimen Batch	No. of Specimen tested	Nom. Strain Rate (%/min)	Uniaxial Compressive Strength (MPa)		Young's Modulus, E1% (MPa)		Young's Modulus E5% (MPa)	
			Avg.	Std. Dev.	Avg.	Std. Dev.	Avg.	Std. Dev.
B7	2	0.007	14	0.5	541	36	268	3
B8	2	0.006	16	0.4	643	1	308	0.5
C9	3	0.0085	17	1.1	533	84	387	40

Table 2.2 Four-point bending test results (Bowders et al., 2003)

Specimen Batch	No of Specimens Tested	Nom. Def. Rate (mm/min)	Flexural Strength (MPa)	Secant Flexural Modulus $E_{1\%}$ (MPa)	Secant Flexural Modulus $E_{5\%}$ (MPa)
A1	13	-	11	779	662
A4	3	4.27	18	1,388	-
A5	3	5.74	11	711	504
A6	4	3.62	10	634	443
B7	1	4.05	9	544	425
B8	1	5.67	-	816	-
C9	2	3.21	12	691	553

Lampo and Nosker (1997) conducted a comparative experimental study on the compressive strength of recycled plastic lumber. During the study, a total of 10 plastic samples were obtained from eight manufacturers. The composition of the product varied greatly, such as some were mixed plastics, some were pure resigns, and others contained fillers such as wood pulp or fiberglass. Lampo and Nosker (1997) performed the experimental study according to ASTM 695-85 with the sample height nearly 12 inches. To calculate the mechanical properties, the study included an effective cross-sectional area which was calculated based on a specific gravity measurement. It should be noted that the compressive strength test was performed at 0.1 in/min rate. Based on the experimental results, the modulus, ultimate strength at 10% strain and yield strength at 2% offset were calculated from the load-displacement data. The specific modulus and specific strength are the moduli divided by specific gravity and the ultimate strength divided by specific gravity, respectively. These "specific" properties display the mechanical properties of the

materials normalized with respect to density during the study. It was expected that the normalization should minimize the effects of voids when comparing the material properties and the effects of different methods of extrusion during the manufacturing process that varied among manufacturers. Based on the study, the compressive strength results are presented in Table 2.3. In addition, the comparisons of compressive strength between different samples are presented in Figure 2.11and Figure 2.12.

Table 2.3 Average values of specific gravity, modulus, specific modulus, yield stress, ultimate stress and specific strength for each sample type (Lampo and Nosker, 1997)

Sample	Specific Gravity	Modulus (MPa)	Specific Modulus (MPa)	Yield Stress (MPa)	Ultimate Strength	Specific Strength (MPa*cm^3/g)
51A	0.2789	262	840	4.89	5.41	19.4
1B	0.7012	427	609	9.52	13.0	18.6
2D (BR)	0.8630	588	682	11.5	16.0	18.5
2D (G)	0.8098	800	988	14.5	19.7	24.3
1E	0.862	557	647	12.2	16.7	19.4
1F	0.7888	746	945	15.1	19.4	24.6
1J(B)	0.7534	643	854	13.1	16.3	21.6
1J(W)	0.9087	759	836	14.9	19.5	21.4
23L	0.7856	1,320	1,680	11.8	13.3	16.9
1M	0.5652	399	705	6.65	8.45	15.0
1S	0.9090	555	610	11.5	14.1	15.5
1T	0.8804	813	921	15.5	21.5	24.4
9U	0.774	598	769	12.6	16.6	21.3

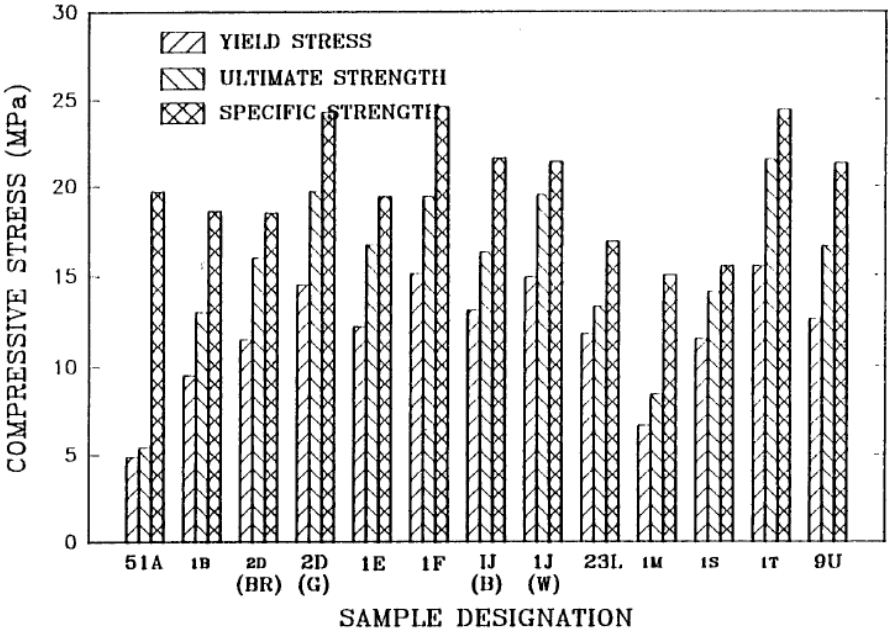

Figure 2.11 Comparison of compressive strength (Lampo and Nosker, 1997)

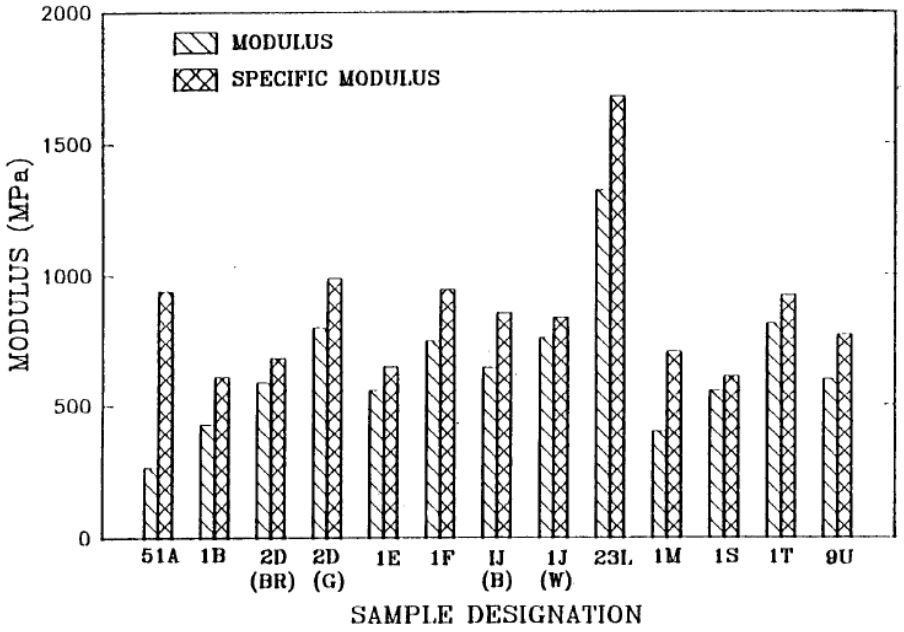

Figure 2.12 Comparison of compressive modulus (Lampo and Nosker, 1997)

Based on the experimental study, Lampo and Nosker (1997) summarized that the values for RPP lumber ranged between 12.0 MPa (1,740 psi) to 24.1 MPa (3,500 psi) for compression and 8.62 MPa (1,250 psi) to 24.1 MPa (3,500 psi) in tension. However, the RPP reached it ultimate strength at different strain level compared to softwood. Breslin et al. (1998) also conducted a comparison between the various test

results observed from the literature as presented in Table 2.4. The study presented that various additives have been incorporated into plastic lumbers (glass fibers, wood fibers, polystyrene) and have shown to increase the stiffness of the lumber.

Table 2.4 Engineering properties of plastic lumber properties (Breslin et al., 1998)

Product	Composition	Compressive Strength (psi)	Modulus of Elasticity (psi)	Tensile Strength (psi)	Source
TRIMAX	HDPE / Glass Fiber	1,740	450,000	1,250	TRIMAX Literature SUNY at Stony Brook
TRIMAX	HDPE / Glass Fiber			1,189	www.lumberlast.com
Lumber Last	Commingled Recycled Plastic	3,755 (ultimate) (D198)	140,000 (D790)	1,453 (ultimate) (D198)	www.ecpl.com
	Post-consumer milk jugs	3,205 (D695)	93,000 – 102,500 (D790)	2,550 (D638)	Zarillo and Lockert (1993)
Earth Care recycle maid Hammer's Plastic	80% HDPE / 20% LDPE	89,814			Zarillo and Lockert (1993)
	HDPE/LDPE (20PSGF)	527,000			
	HDPE / LDPE (40PS20GF)	653,000 (D790)	1,793 (D638)		
Superwood Selma, Alabama	33% HDPE / 33% PP	3,468 (D695)	146,171 (D790)	1,793 (D638)	
California Recycling Company	100% Commingled	81,717			Beck, R. (1993)
	10% PP / 50% HDPE	79,319			
RPL-A	HDPE / Glass Fiber	92,636 (D790) 2,000			Smith and Kyanka (1994)

Product	Composition	Compressive Strength (psi)	Modulus of Elasticity (psi)	Tensile Strength (psi)	Source
RPL-B	49% HDPE / 51% Wood Fiber				Smith and Kyanka (1994)
Rutgers University	100% Curb tailings	3,049	89,500		Renfee et al. (1989)
	60% Milk bottles, 15% Detergent bottles, 15% Curb tailings, 10% LDPE				Renfee et al. (1989)
	50% Milk bottles, 50% Densified PS	4,120 (D695)	164,000 (D790)		Renfee et al. (1989)
Earth Care Products	HDPE		173,439 (D790)		www.ecpl.com
BTW Recycled Plastic Lumber	Post-Consumer	1,840-2,801	162,000		BTW/Hammers Brochure

Plastic is a temperature dependent material. At low temperature, the plastic is robust and brittle. With the increase in temperature, the plastic becomes weaker and become more ductile. Malcolm, M. G. (1995) presented the effect of temperature change on the tensile strength of HDPE materials as presented in Figure 2.13.

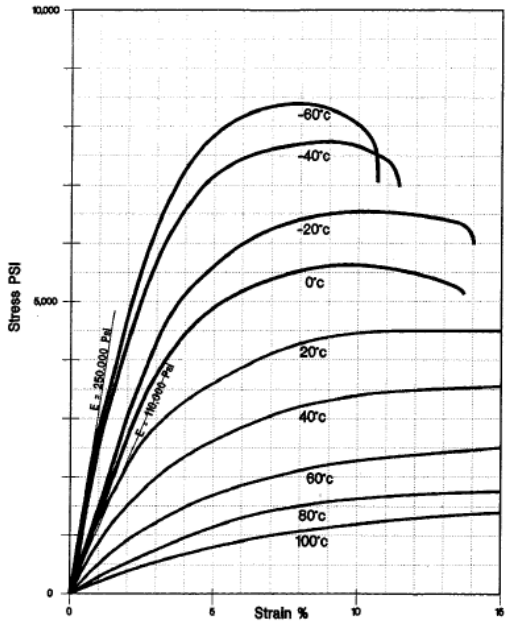

Figure 2.13 Tensile strength of HDPE (Malcolm, M. G.,1995)

A total of 9 RPP samples were tested to evaluate the flexural strength, using 3-point bending test in accordance with ASTM D790. Loehr and Bowders, (2007) presented that stress and stiffness of RPP are sensitive to loading rate. Bowders et al. (2003) conducted an experimental study of RPP for slope stabilization where the deformation rates were utilized 5 to 10 times lower than the suggested value in ASTM D6109. Since the loading rate in slope stabilization is much lower than the suggested loading rate in accordance to ASTM D790, the 3-point bending test was conducted at 3 different loading rates (0.5 kips/min, 2.7 kips/min and 4.9 kips/min) that ranged between the ASTM D790 and suggested loading rate for slope stabilization. A total of 3 samples were tested for each loading rate. The stress-strain response at different loading rates is presented in Figure 2.14. The flexural strength and elastic modulus of RPP ranged between 3.1 to 4.7 ksi and 190 to 200 ksi, respectively. The experimental results were further utilized for the design of slope remediation.

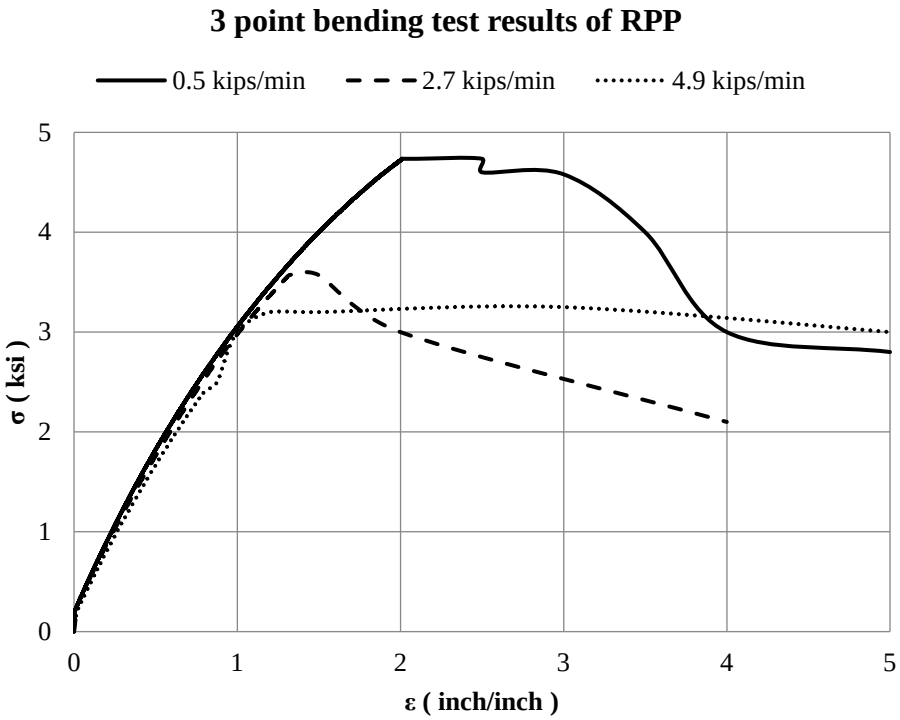

Figure 2.14 Stress-Strain Response of RPP at Different Loading Rates

Chapter 3: Laboratory Testing of Yazoo Clay Soil

3.1 Introduction

The laboratory testing program was designed to determine properties relating to volume change behaviors of expansive Yazoo clay soils. A Highway slope located on in Jackson Mississippi has been selected for this study. Representative Yazoo clays soil samples collected from Geotechnical Engineering Company Burns Cooley and Dennis in Ridgeland; MS were collected and are investigated at the laboratory. The experimental program was mainly comprised of tests to determine basic soil properties, such as sieve analysis, hydrometer tests and Atterberg limits test, and engineering characteristics, including directional test and total soil suction measurement test. A brief summary of the laboratory procedures, equipment used and results obtained are presented in the following sections. All representative soil samples were subjected to various physical property measurements.

3.2 Atterberg Limits Test

It has been found that the water contents corresponding to the transitions from one state to another usually differ for clays having different physical properties in the remolded state, and are approximately equal for clays having similar physical properties. Therefore, the limiting water contents, or limits, may serve as index properties useful in the classification of clays. As the soil-water mixture passes from one state to another, there is no abrupt change in the physical properties. The Atterberg limit tests, therefore, are arbitrary tests that have been adopted to define the limiting values. The Atterberg limits vary with the amount of clay present, the type of clay mineral, and the nature of the ions adsorbed on the clay surface. Unlike finer soil particles, gravels and sands do not possess the required cohesiveness which permits the Atterberg limits tests to be performed. However, the finer sands and silts often contain sufficient clay coatings to allow the tests to be successfully completed.

Atterberg tests are performed on only that soil fraction which passes through a No. 40 sieve (0.425 mm). Consistency limits (LL and PL) are significant to understand the stress history and general properties of the soil met with construction. An estimate of Plasticity Index is necessary to classify the soils, particularly in highly expansive clays. The Atterberg Limit test was performed in the Geotechnical Engineering Laboratory at Jackson State University. The test was conducted according to ASTM D4318. The moisture content of the soil samples for the liquid limit test is presented in Figure 3.1.

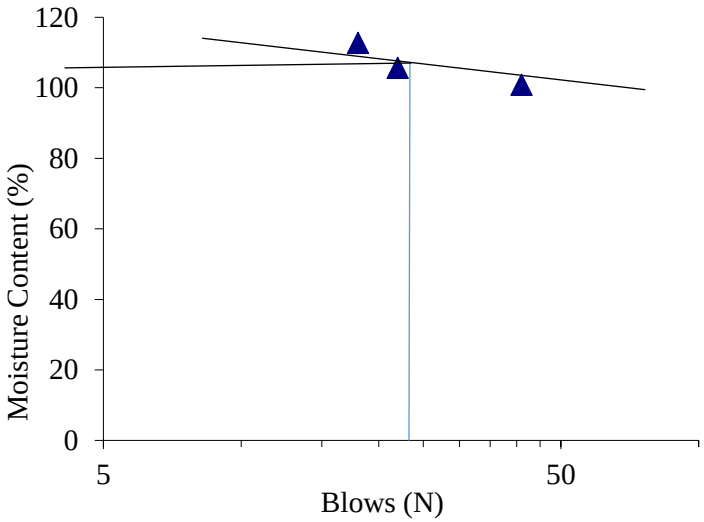

Figure 3.1 Graph of Liquid Limit Test

From the chart, Liquid Limit equals 108% at 25 number of blows. It is observed that the highest percentage of moisture content is 112.7 which is dependent on the number of blows N. It can be inferred that the higher the number of blows N, the lower the moisture content. This dependency is seen on the resulting graph, a linear graph (Figure 3.1). From the graph, the moisture content at which Yazoo clay soil will tend to behave like a plastic material is determined at 25 number of blow count as 108, which is the Liquid Limit (LL). The plasticity index of 84 was calculated, which is high and provides a clue that the sample is likely clay. In the grain-size classification, soils are designated according to the grain-size or particle-size. Terms such as gravel, sand, silt, and clay are used to indicate certain ranges of grain-sizes. Modern engineering classification systems are designed to allow an easy transition from field observations to basic predictions of soil engineering properties and behaviors. The soil is classified using ASHTOO classification system chart as inorganic clay of high plasticity (CH).

3.3 Sieve Analysis Test

Most granular soils and fine aggregates are mixtures of desirable coarse particles, sand, and undesirable clay or plastic fines. The sieve analysis test (Figure 3.2) which can also be referred as grain size test or sand equivalent test is intended as a rapid field correlation test to indicate the relative proportions of clay-like or plastic fines and dust in granular soils and fine aggregates that pass the No. 4 (4.75 mm) sieve size. The test assigns an empirical value to the relative amount, fineness, and character of clay-like material present in a soil sample. At first, the sieve analysis test was performed according to ASTM C136. Later the retained soil over #200 U.S. sieve (75μm sieve opening) was washed according to ASTM D1140 (wash sieving) test method. The Yazoo clay soil has 96.8% passing No. 200 sieve. Therefore, hydrometer test is conducted to investigate the grain size distribution of fine content.

Figure 3.2 Sieve analysis at the Geotechnical Engineering Laboratory

3.4 Hydrometer Test

The hydrometer analysis, also called sedimentation method because it is based on the principle of sedimentation of soils in water. It is used to determine the grain size distribution for a fraction of the soil that is smaller than the No. 10 sieve. Fine soil particles are dispersed by soaking the soil sample in a dispersing agent and by rapid stirring to neutralize the charges between the soil particles. The test (Figure 3.3) uses a Type 152H calibrated hydrometer to give the mass of solids with a specific gravity equal to 2.65 in suspension and the settling velocity of the dispersed soil particles. Hydrometer test is used to determine what type of clay is predominant in a given soil sample (e.g.: kaolinite, illite, montmorillonite, etc.). The hydrometer test was performed according to ASTM D7928-17 test method. The combined particle size distribution curve of the Yazoo clay soil is presented in Figure 3.4.

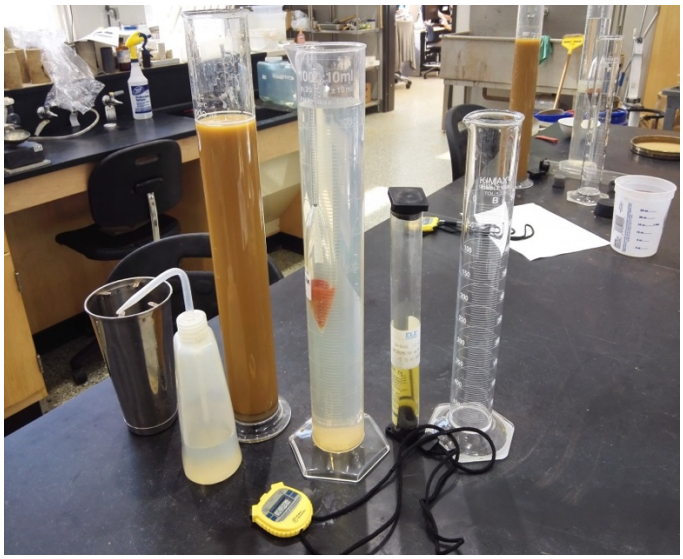

Figure 3.3 Hydrometer Test

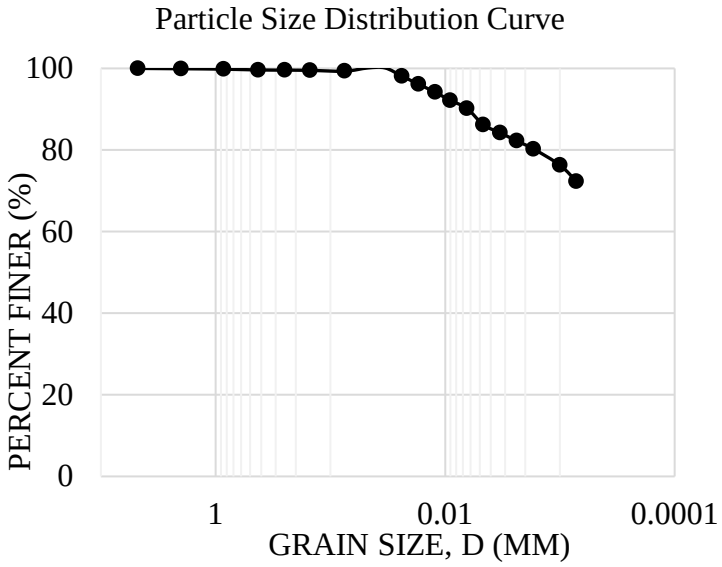

Figure 3.4 Combined Particle Size Distribution Curve of Yazoo Clay soil

In Figure 3.4, the particle size distribution curve shows values ranging from 0.068mm to 0.00095mm. It can be inferred from the hydrometer readings, that the highest particle settlement occurred between 2 – 4mins which gave a hydrometer reading of 46 and 31 respectively. This resulted to a steep slope noticed in the graph with a corresponding effective length difference of 2.4mm. Also, it can be induced that the soil particles settled to the bottom of the 1000ml cylinder in an ascending (i.e.; particles with smaller diameter settles first leaving those with bigger diameter on top) order of its size particles and reflected on the graph, showing a steady increase in slope up to the point the big effective length difference was experienced.

3.5 Soil Water Characteristics Curve using Filter Paper Method

The filter paper method (according to ASTM D5298 – 16) is a soil suction measurement technique used to determine the moisture condition of unsaturated soils. This test allows for both the matric suction and total suction to be measured. During this test, if the filter paper is allowed to absorb water through fluid flow (contact method), then only matric suction is measured the filter paper is allowed to absorb water through vapor flow (non-contact method), then only total suction is measured. Different samples were prepared of various water contents. A filter paper 5.5cm Whatman 42 filter paper is sandwiched between two bigger 7.7cm size protective filter papers, inserted between each sample and held together by the use of electric tape for matric suction measurement. The sample is then put inside a plastic jar. To measure the total suction measurement, a ring type support (2 cm in height) was kept on top of the soil to provide a non-contact system between the filter paper and the soil inside the jar. The jar was air tightened and was placed in a temperature controlled environment for 8 days before the moisture content for both the matric and total suction measurements were determined. After obtaining all of the filter paper water content values using a 0.0001g accuracy weighing scale, a wetting calibration curve was employed to get matric and total suction values of the soil samples, as presented in Figure 3.5.

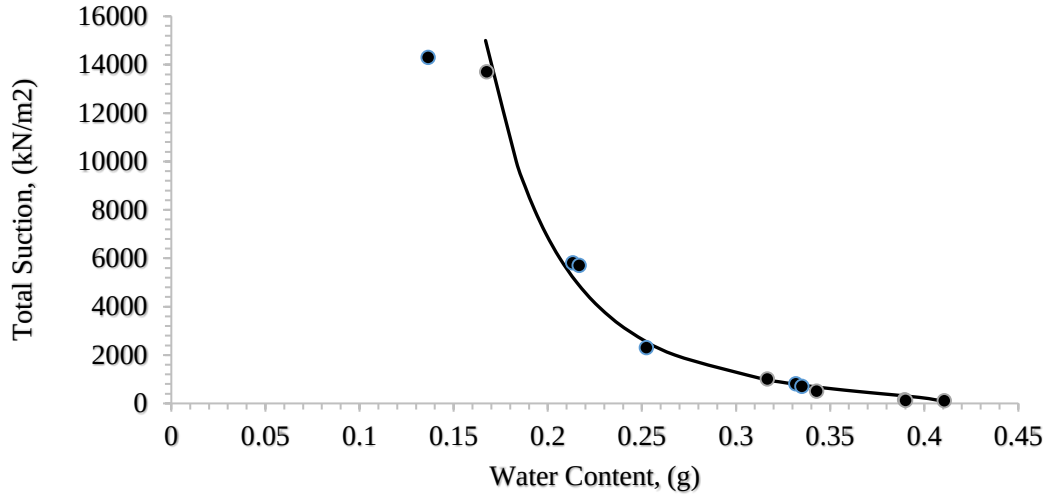

Figure 3.5 SWCC Curve

3.6 Direct Shear Test

This test method covers the determination of the consolidated drained shear strength of cohesive Yazoo clay soil in direct shear. The direct shear test is performed following the ASTM D-3080 standard by deforming a specimen at a controlled strain rate on or near a single shear plane determined by the configuration of the Geojac direct shear apparatus. Some test photos are presented in Figure 3.6. Generally, three or more specimens are tested, each under a different normal load, to determine the effects of shear resistance and displacement, and strength properties such as Mohr-Coulomb strength envelopes. Normal loads of 25KPa, 50KPa, and 100KPa is applied to three different Yazoo clay soil samples of 2.5-inch diameter and 1 inch in height.

Based on the direct shear test results, the peak shear strength of the samples with the applied normal stress is plotted to develop the Mohr-Coulomb failure envelope, as presented in Figure 3.7. As presented in the failure envelope, the friction angle ϕ (18.7 degrees) and cohesion c (5.221KPa) is determined.

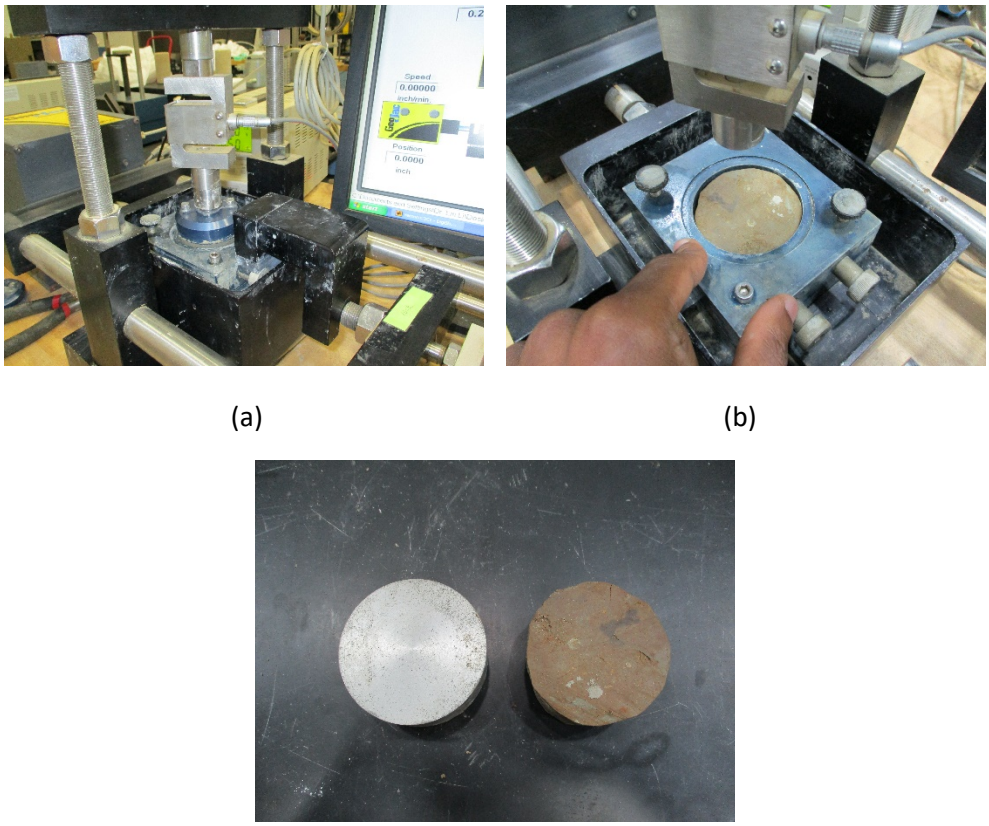

Figure 3.6 (a) Direct Shear Test (b) Soil Sample mold (c) Soil Sample

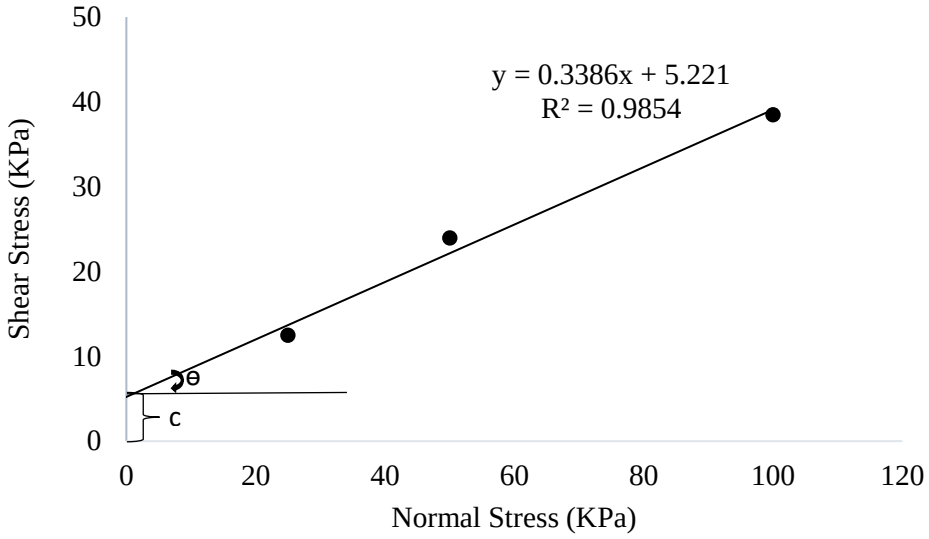

Figure 3.7 Graph of Shear Stress versus Normal Stress

Chapter 4: Effect of Rainfall on Slope Failure

4.1 Introduction

Slopes and embankments are one of the major components of the maritime and multimodal transportation infrastructure, which often subjected to shallow landslides due to the existence of expansive clay soil. Yazoo clay soil is highly expansive in nature and extended over central Mississippi, Alabama, and Southern Louisiana. Shallow slope failures are frequent in embankments constructed on expansive Yazoo clay in Mississippi due to the rainfall volume and climatic variation. In Mississippi, the shallow slope failure on Yazoo clay soil is induced by the climate variation, generally considered as temperature and rainfall, and require the significant budget to be repaired. Moreover, if the shallow failures are not properly maintained, it requires more extensive and expensive repairs (Loehr and Bowders, 2007; Loehr et al., 2007, Hossain et al., 2017). Typically, shallow slope failure occurs due to an increase in pore water pressure and reduction of soil strength due to progressive wetting of soil near-surface soil (Khan et al., 2017). This condition further intensified by moisture variation due to seasonal climate change that results in cyclic shrink and swell of the high plastic clay soils. The possible cause of slope failure is defined by penetration of rainwater into the cracks, which generate a softened zone in the soil slope (Hossain et al., 2012). Rainfall-induced slope failures are reported to occur during or immediately following periods of intense or prolonged heavy rainfall in fine-grained soil (Day, R. W. 1989, Tohari et al., 2007). The unsaturated state of the soil plays a major role in protecting natural slopes from failure. With even a minimal amount of suction, the shallow soil deposit often has a high factor of safety, depending on slope morphology and the triggering of a landslide is not a common phenomenon (Damiano and Mercogliano, 2013). Moreover, the soil covers often offer a low hydraulic conductivity at unsaturated state that usually prevents the soil from approaching saturation even during the high-intensity rainfall period and protects the soil to be fully saturated due to rainfall.

This chapter summarizes the effect of rainfall on the factor of safety of fill slopes constructed with Yazoo clay soil was investigated using Finite Element Method (FEM). The historical rainfall pattern of Mississippi from NOAA is evaluated and different intensity (2 mm/ hour to 50 mm/hour) and duration of precipitation (30 mins to 7 days) are selected, based on a return period of 50 years, 100 years and 500 years. Three fill slopes constructed on Yazoo clay soil with slope ratios of 2H: 1V, 3H: 1V and 4H: 1V are selected. Based on more than 150 unsaturated finite element analysis results, the variation of suction under rainfall is investigated using coupled flow-deformation analysis.

4.2 Precipitation Pattern

NOAA collects the rainfall data all over the US and develops the precipitation pattern of any locality based on the historical data (NOAA Atlas 2014). The PDS based intensity duration and frequency (IDF) curve of precipitation, based on NOAA Atlas 2014 of Jackson, Mississippi, was collected. The IDF curve of Jackson Area is presented in Figure 4.1, which indicated that the high-intensity rainfall ranges between 234.95 mm/hour (for 15 mins. duration) and 21.844 mm/hour (for 12 hours duration) with a 500-year return period.

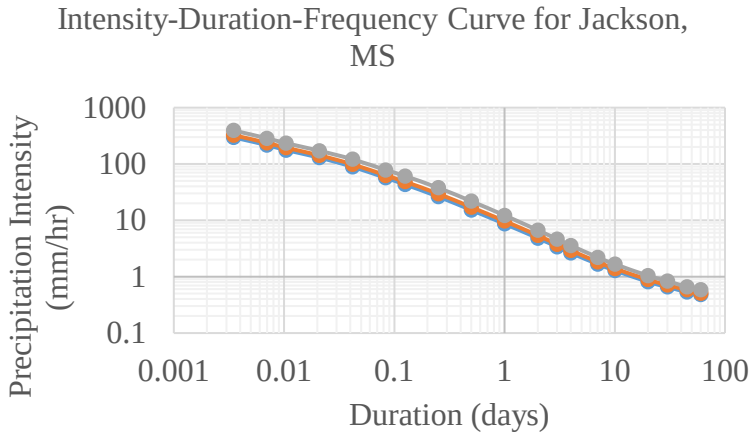

Figure 4.1 PDS based intensity duration frequency (IDF) curves for Jackson MS

Different intensity (63.5 mm to 373.38 mm) and duration of rainfall (30 mins to 7 days) are selected, based on a return period of 50 years, 100 years and 500 years, from the PDS based IDF curve of Jackson, MS. Moreover, three fill slopes constructed on Yazoo clay soil with slope ratios of 2H: 1V, 3H: 1V and 4H: 1V are selected. The FEM matrix for the selected slope inclinations and rainfall intensities are presented in Table 4.1.

Table 4.1 Selected Precipitation pattern for FEM analysis

Slope Inclination	**Duration**	**Rainfall Intensity (mm/hr.)**		
		50 Years Return Period	100 Years Return Period	500 Years Return Period
2H:1V, 3H:1V and 4H:1V	30-min	63.5	70.87	85.85
	60-min	88.9	98.55	122.17
	2-hr	113.28	126.24	158.24
	6-hr	158.75	178.82	229.87
	12-hr	184.65	207.52	264.16
	1 day	209.55	234.18	294.64
	3 day	246.88	271.78	335.28
	7 day	284.48	312.42	373.38

4.3 Laboratory Investigation of Yazoo Clay Soil

A Highway slope located on in Jackson Mississippi has been selected for this study. Yazoo clays soil samples from the slope sites are investigated at the laboratory to determine the physical properties such as liquid limit, plasticity index, grain size analysis, hydrometer and unit weight. The laboratory testing program was designed to determine physical properties of soil. The liquid boundary of the Yazoo clay was 108 and Plasticity Index was 84. The peak shear strength of the expansive Yazoo clay was determined in

the laboratory investigation program which indicated that the cohesion and friction angle are 5.221 (kN/m2) and 18.7 respectively. The soil water characteristic curve (SWCC) of the Yazoo clay soil that investigates the unsaturated behavior is developed and presented in Figure 4.2, which the Van Genuchten fitting parameters (α, m and n) and residual and saturated water content (θ_s and θ_r) parameters were obtained (V Genuchten, 1980). The SWCC is developed using filter paper method as suggested by Bulut et al., 2001.

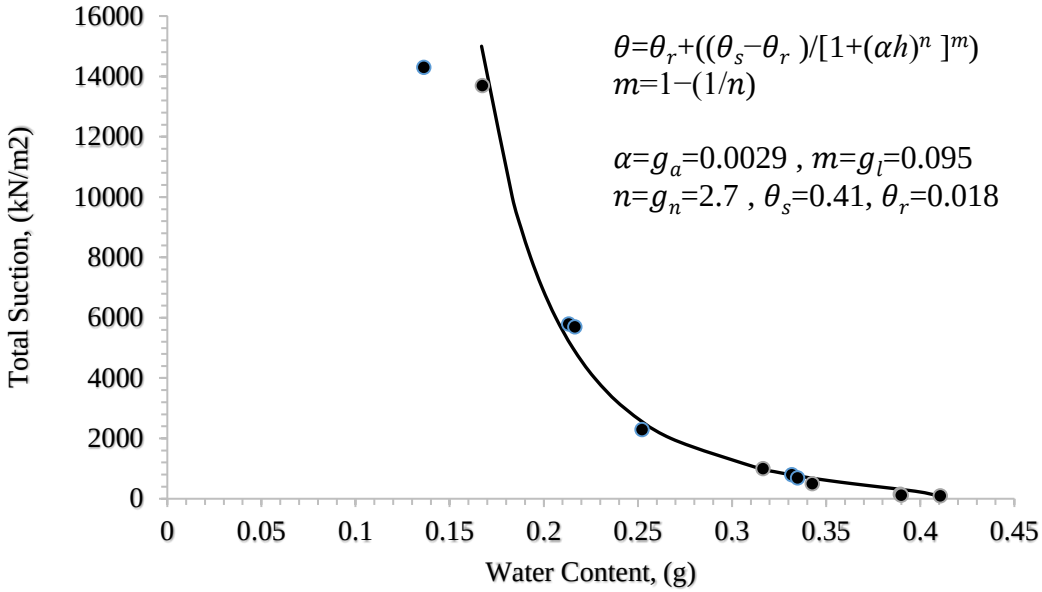

Figure 4.2 Soil-water characteristic scatters graph with the Fitting curve

4.4 Methodology and Approach: Finite Element Model

The FEM program PLAXIS 2D was used to conduct the coupled flow-deformation analysis. A 15-node triangular element was used, which provides a fourth order interpolation for displacements, and the numerical integration involves twelve Gauss points. The Van Genuchten model is considered as the hydraulic model. The soil parameters, as shown in Table 4.2, were used in the numerical analysis using PLAXIS 2D. They were established from existing soil test reports. Precipitation of different intensities was applied to the soil model to assess the flow behavior during rainfall. The analysis was carried out at three rainfall intensities. The rainfall intensities were selected based on 50, 100, and 500-year periods of Mississippi rainfall data. The flow through the top soil was determined for each of the intensities assuming rainfall durations lasting 30 min, 60 min, 2 hours, 6 hours, 12 hours, 1 day, 3 days and 7 days. The representative soil model is presented in Figure 4.3. The boundary condition as outlined in the figure is infiltration for top soil which allows simulating water ponding at the top soil. During the dry period, the highly plastic clay soil developed desiccation cracks which might have significantly increased the permeability along the vertical direction of the top soil at the active zone. However, due to the desiccation crack, the permeability along the horizontal direction might have had no effect and could have remained unchanged (Khan et al., 2017). Therefore, a high vertical permeability value of ky = 1.063 m/day ($1.23 * 10^{-5}$ m/s) was used for the top mentioned part for each one of slopes to simulate the effect of the desiccation crack, as suggested by Khan et al., 2017. In other clay layers, the permeability for both horizontal and

vertical directions was selected as 0.0475 m/day ($5.5 * 10^{-7}$ m/s). The water table was placed at 3 m (10 ft), below the ground surface.

Table 4.2 Soil parameters for FEM analysis

Parameter	Name	Unit	Soil 1	Soil 2	Soil 3	Soil 4
Bulk unit weight	Υ_{unsat}	kN/m^3	19.6	19.6	20.5	22
Saturated unit weight	Υ_{sat}	kN/m^3	21	21	22	22
Horizontal permeability	k_x	m/day	5.50E-07	5.50E-07	5.50E-07	5.50E-07
Vertical permeability	k_y	m/day	1.23E-05	5.50E-07	5.50E-07	5.50E-07
Residual water content	S_{res}	-	0.018	0.018	0.018	0.018
Saturated water content	S_{sat}	-	0.41	0.41	0.41	0.41
Van Genuchten fitting parameter	$n=g_n$	-	2.7	2.7	2.7	2.7
Van Genuchten fitting parameter	$\alpha=g_a$	1/m	2.90E-03	2.90E-03	2.90E-03	2.90E-03
Van Genuchten fitting parameter	$m=g_l$	-	0.095	0.095	0.095	0.095
Cohesion	C	kN/m^2	5.221	4.788	11.97	143.640
Friction angle	Φ	-	18.7	23	15	35

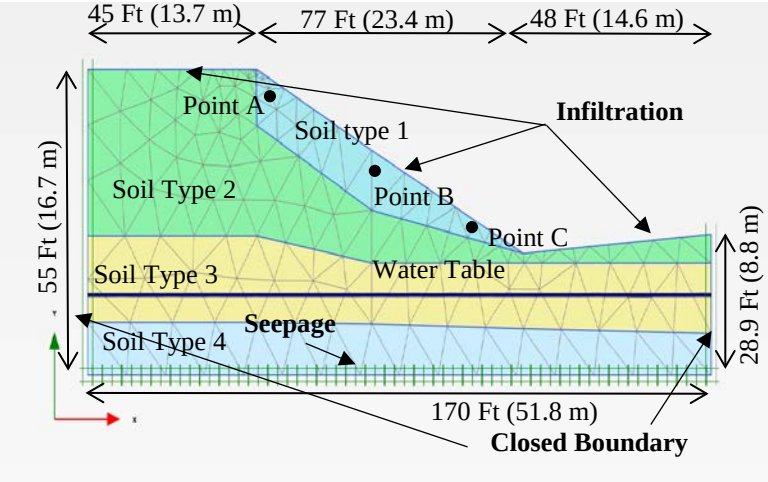

Figure 4.3 The boundary conditions for the soil flow model

4.5 Finite Element Modeling Results

The variations of suction at the crest of the slope for the slope 2H: 1V for 2 hrs, 1 day and 7 days rainfall intensities are presented in Figure 4.4 (a) to (l). As it is indicated, that the suction immediately dropped at the top of the slope after rainfall for the three slopes and continued to drop during rainfall, representing the accumulation of water at the corresponding depth. It is also observed that the suction decrease is continued for few hours, even after the rainfall, which has taken place due to the water ponding at the top for all three slopes (Figure 4.4(c), (g) and (k)). It is also noticed that after few days of rainfall, the suction increased and it almost regained its original profile for steeper slope. However, (Figure 4.4(l)), virtually no suction variation occurred throughout the slope except a small amount of increase at the very top crest of the slope at flatter slope.

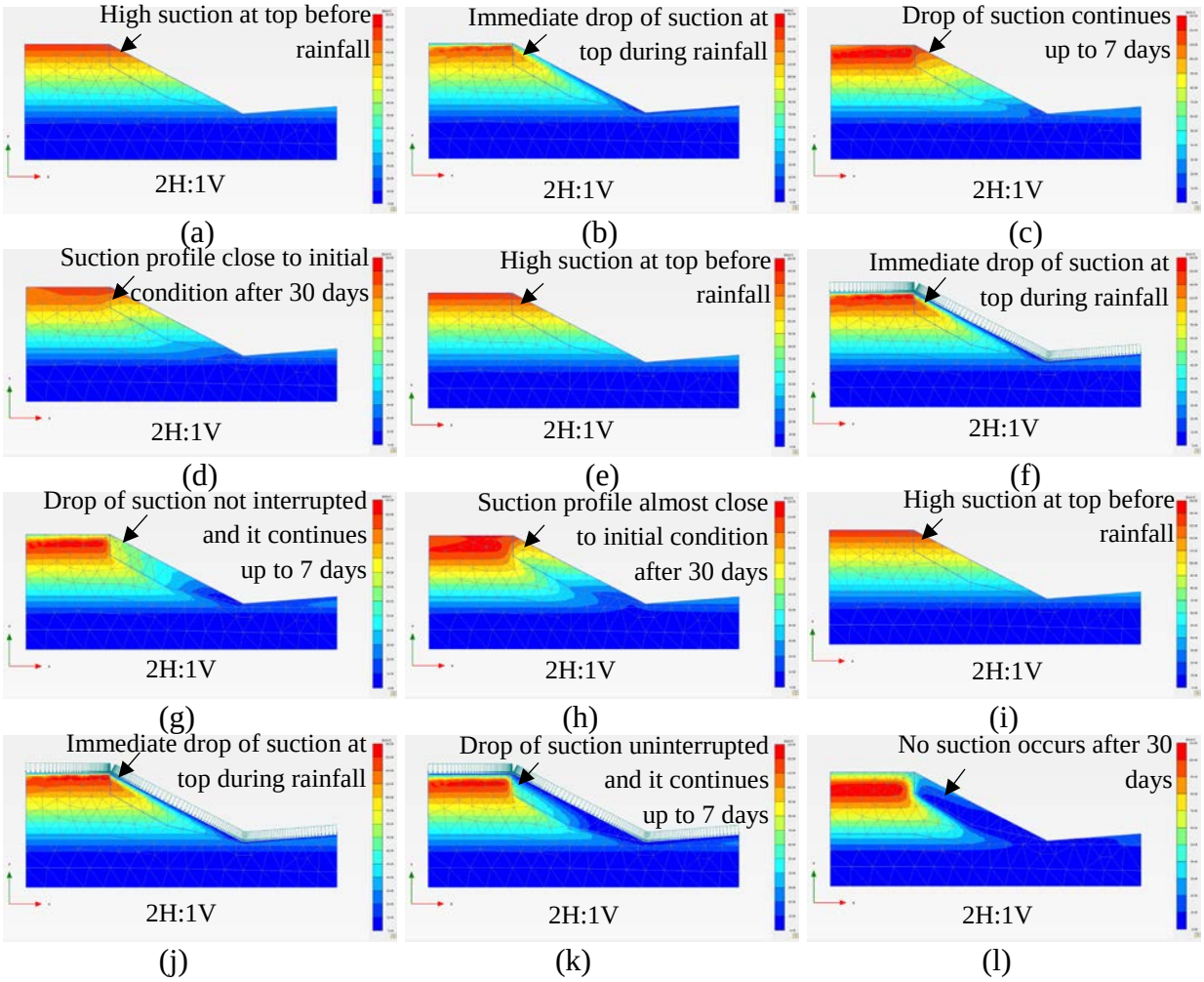

Figure 4.4 Suction profile for 2 hrs rainfall intensity (a) prior to rainfall (b) during rainfall (1 day) (c) 7 days after rainfall (d) 30 days after rainfall, Suction profile for 1 Day rainfall intensity (e) prior to rainfall (f) during rainfall (1 day) (g) 7 day

It should be noted that during the FEM analysis, infiltration boundary was used at the top soil, which allowed ponding of water to simulate realistic behavior. The ponding status is established when the rainfall intensity is equal to the infiltration capacity. From FEM analysis results, it can be seen that ponding occurrence exists in almost all surficial soil for three slope ratios in 30 min and 60 min rainfall intensities. But, for 6-hrs rainfall intensity, ponding condition can be found hardly at the slope, due to the low intensities. In particular, ponding has affected the matric suction according to the mentioned rainfall intensities. In other words, ponding occurrence decrease amount of suction at the top soil. As illustrated in Figure 4.5, the ponding is mostly existing in the toe of the slope.

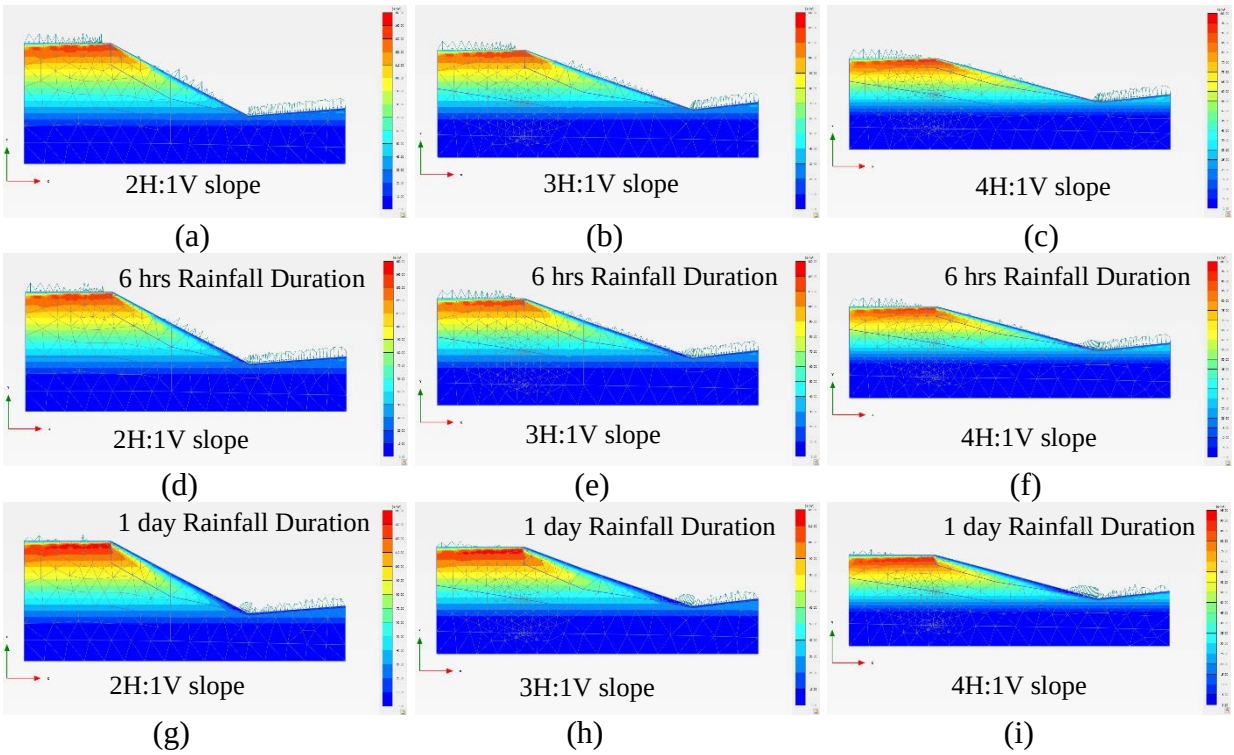

Figure 4.5 Ponding occurrence for 30 min rainfall intensity (a) 2H:1V (b) 3H:1V (c) 4H:1V, Ponding occurrence for 60 min rainfall intensity (d) 2H:1V (e) 3H:1V (f) 4H:1V and Ponding occurrence for 6 hrs rainfall intensity (g) 2H:1V (h) 3H:1V (i) 4H:1V

The variations of change in suction versus time due to the 8 rainfall durations at 100 years return period for 3 slope ratios at point A (a) to (c) are presented in Figure 4.6. It should be noted that Point A is located at the crest. Moreover, the point A, B, and C is located at the surface, and it is worth mentioning that variation of change in suction due to the 8 rainfall durations at 100 years return period for the three slopes at points B and C have the same trend. The change of suction refers to the change from the initial suction value prior to rainfall.

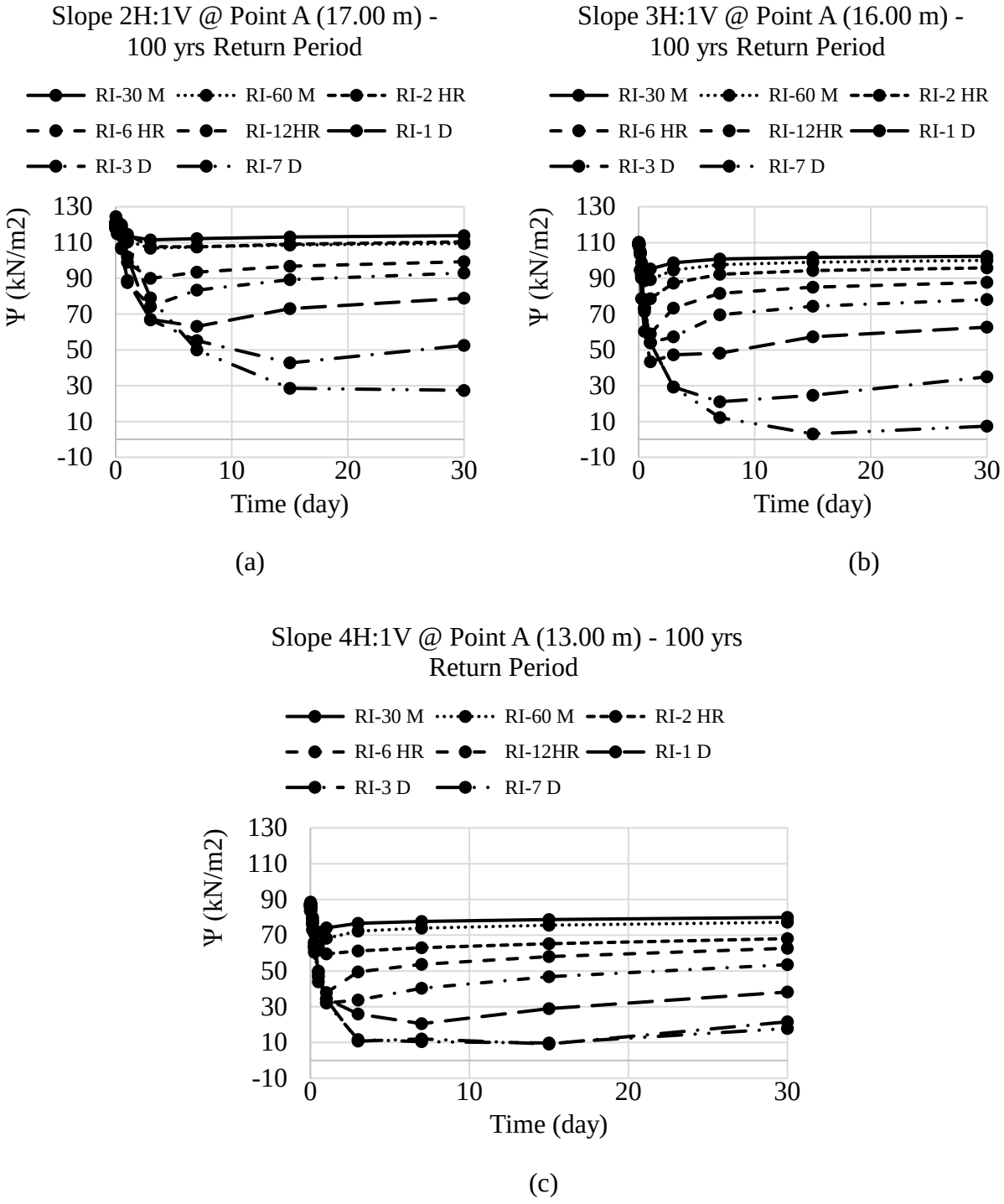

Figure 4.6 Variations of change in suction versus time for 8 rainfall durations at 100 years return period for 3 slope ratios at point A, (a) 2H:1V, (b) 3H:1V and (C) 4H:1V

Based on Figure 4.6, the change in suction was more significant at the initial period, whereas it starts decreasing with the milder slope. The maximum change in suction was observed at the steeper slope (2H:1V) that the flatter slope (4H:1V). For example, the matric suction value is about 130 kPa for 2H:1V slope, which is higher than the matric suction values are 110 kPa and 90 kPa for 3H:1V and 4H:1V slope

ratios respectively. As it seen, the matric suction value of the crest dropped from 130 kN/m^2 to 90 kN/m^2 on the first day of rainfall. The figure shows various rainfall durations with a 100-year return period. The suction was observed to drop remarkably with higher intensity and longer duration of rainfall, and it continues with slight changes. Moreover, the change in suction was more significant at the crest of the slope, when compared to the middle and toe of the slope. The drop of suction was instantaneous at the depth for different rainfall intensities and durations, as depicted in Figure 4.6. In contrast, the change in suction continued several days to weeks post-rainfall to reach a steady value at point A in depth. The constant values of suction at the crest of the slope (point A), indicated that the water that is moved and filtered in porous voids (percolation theory) could not drain out from the slope due to the low permeability of the highly. Figure 4.7presents the suction profile for low (60 min), medium (1 day) and high (7 days) rainfall intensities for three slope ratios 2H:1V, 3H:1V and 4H:1V. The FEM analysis results indicated that for three slope ratios, at low rainfall intensity suction dropped immediately at surficial soil, and drop of suction uninterrupted for 1-day rainfall intensity, and it continued until there was no significant suction occurrence at high rainfall intensity such as 7 days. It should be noted that the change in suction was more notable at a lower depth (point A) to the longer period of high rainfall intensity for almost all three slope ratios. The change in suction was not substantial at point B or C.

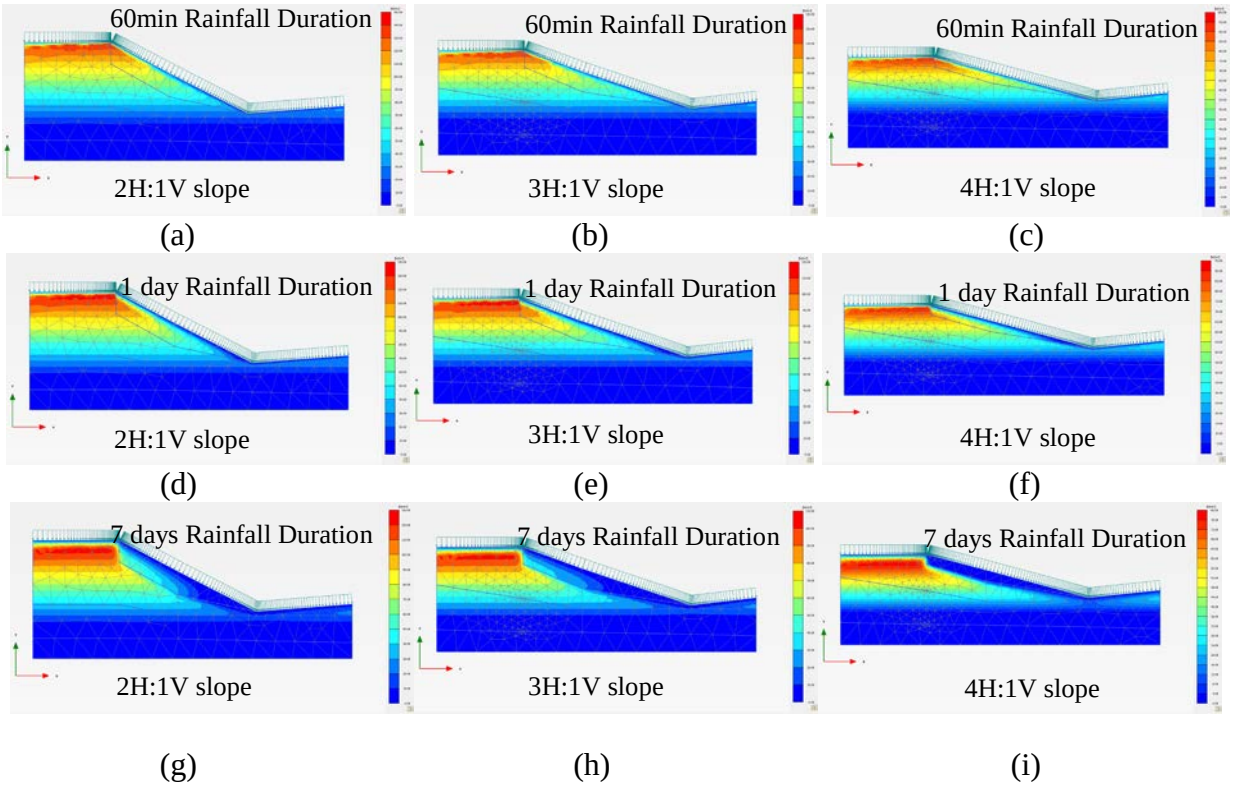

Figure 4.7 Low rainfall intensity suction profile (a) 2H:1V (b) 3H:1V (c) 4H:1V, Suction profile for medium rainfall intensity (d) 2H:1V (e) 3H:1V (f) 4H:1V and Suction profile for high rainfall intensity (g) 2H:1V (h) 3H:1V (i) 4H:1V

4.6 Stability Analysis Results

The factor of safety of a slope is defined based on shear strength reduction method as the factor in which the original shear strength parameters can be reduced in order to bring the slope to the point of failure

(Griffith and Lane, 1999). During this study, stability analysis was conducted considering the unsaturated moisture and matric suction variation of the soil, as investigated by the flow analysis. The slip surface of low (2 hrs), medium (1 day) and high (7 days) rainfall intensities for three slope ratios 2H:1V, 3H:1V and 4H:1V are presented in Figure 4.8. Based on FEM results, it can also be observed that the factor of safety changed slightly with the increase of rainfall intensity for different rainfall durations. The factor of safety of the three slope ratios 2H:1V, 3H:1V and 4H:1V were observed approximately as 1.5, 1.8 and 2.2 respectively. The amount of factor of safety indicates that the slope is stable even in fully-softened condition with the presence of matric suction. In addition, all the failure surface is observed as deep-seated, which occurred due to the presence of matric suction. As the rainfall in influencing the matric suction value at the top soil, almost no change in the factor of safety occurred in deep-seated failure.

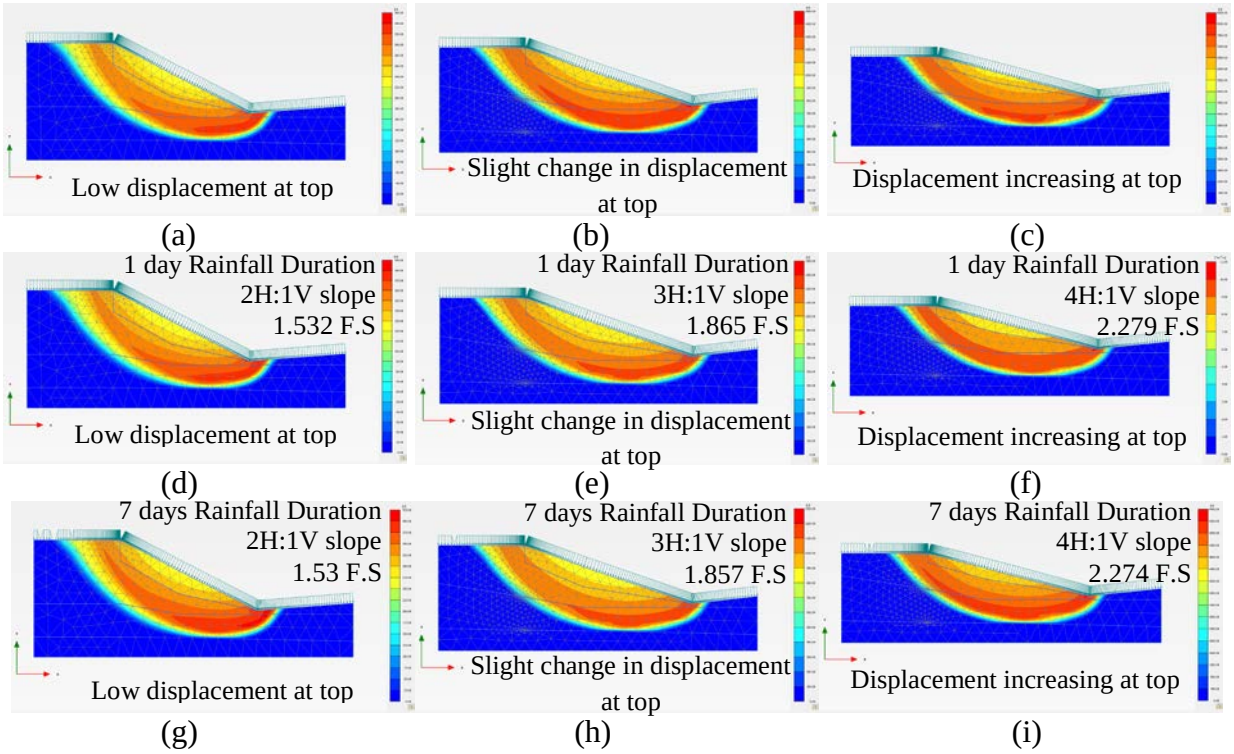

Figure 4.8 Total displacement change for low rainfall intensity-2 hrs (a) 2H:1V (b) 3H:1V (c) 4H:1V, for medium rainfall intensity-1 Day (d) 2H:1V (e) 3H:1V (f) 4H:1V and for high rainfall intensity-7 Days (g) 2H:1V (h) 3H:1V (i) 4H:1V

4.7 Effect of Suction on Shallow Slope failure

Usually, rainfall-induced slope failures in Mississippi area are shallow in nature, where the failure depth is ranged within 6-8 ft. depth. However, at different rainfall intensities and durations, the three slopes experienced deep-seated slope failure, as depicted in Figure 9**.** Khan et al., 2017 conducted a failure investigation of in highway slope on expansive soil which indicated that the failure of the slope induced by the formation of perched water condition due to rainfall. An additional analysis was conducted with a perched water in the fully softened soil and ignoring matric suction in the same slope to simulate the similar behavior. It is interesting to observe that the slip surface become shallow, where the factor of safety of the slope immediately dropped from 1.86 to 1.08, as presented in Figure 4.9. This clearly indicates that a small presence of the matric suction restricts the shallow slope failure and increase the factor of safety of the

slope significantly. Moreover, it can be concluded that the simulated rainfall did not saturate enough in the slope to substantially reduce the matric suction, as presented in the previous section. In real time, the rainfall takes place several times during the wet period, which progressively reduces the matric suction of the soil. Further analysis was conducted on the 3:1 slope to simulate the effect of the continuous rainfall on the matric suction. The actual rainfall for the month of June 2016 at Jackson, MS is selected and then applied at the rainfall to investigate the successive effect of rainfall. The variation of change in suction for different rainfall durations for 3H: 1V slope based on progressive rainfall condition in Jackson, MS are presented in Figure 4.10(a) to (f). The increasing rainfall intensity is shown in Figure 4.10 (a). The variation of change in suction is obtained as it is depicted in Figure 4.10(b) to (f). It is observed that with the continuous rainfall the suction dropped significantly due to several rainfalls events in series. As a result, the slope failure in shallow depth likely happens to the surficial soil.

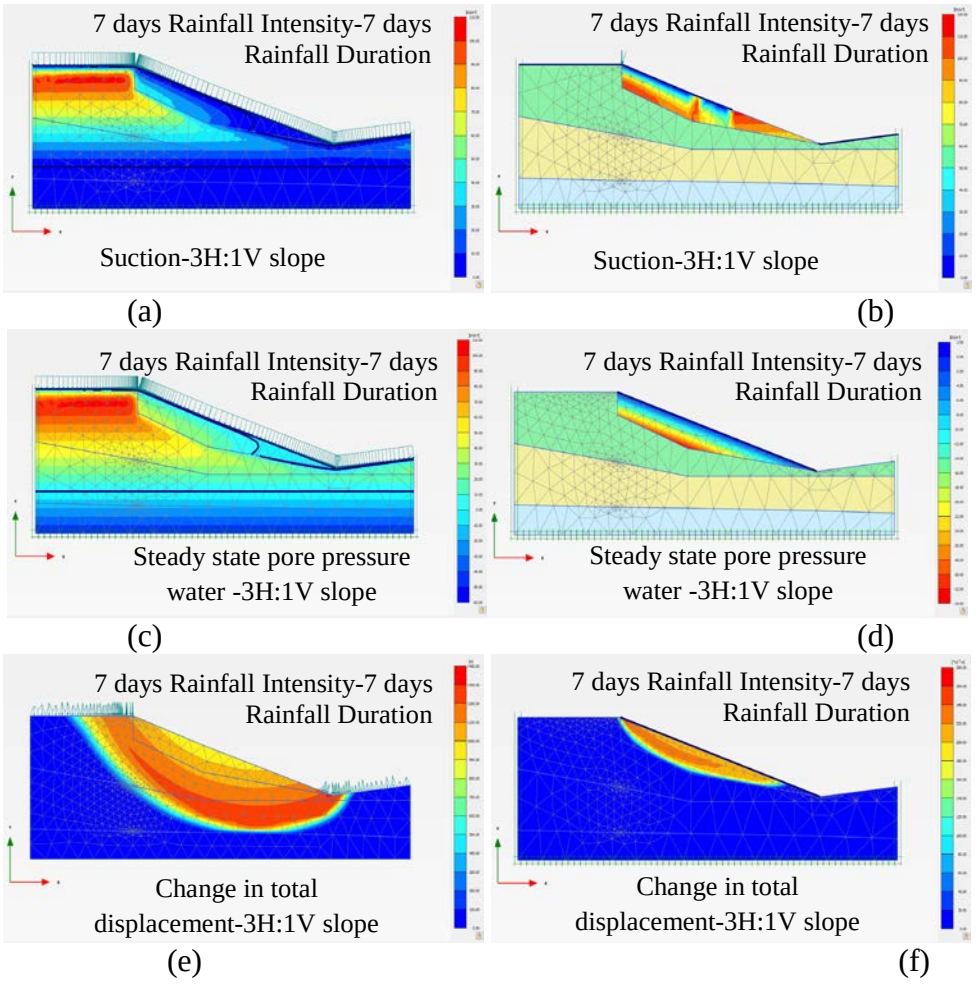

Figure 4.9 (a) Deep slope failure suction change (b) shallow slope failure suction change (c) Steady-state pore pressure water for deep slope failure (d) Steady-state pore pressure water for shallow slope failure (e) Deep-seated slip surface condition (f) Shallow

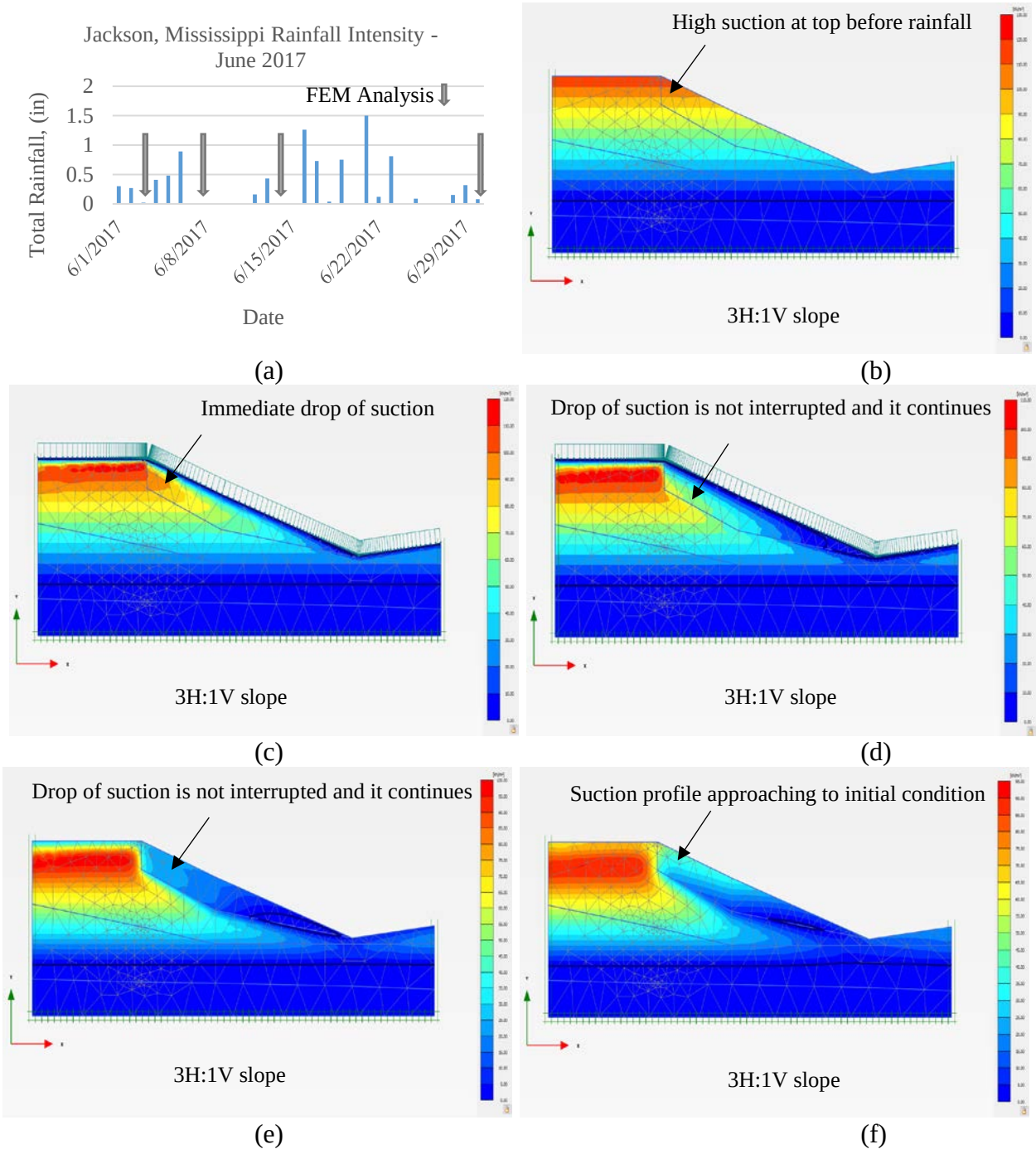

Figure 4.10 (a) Rainfall intensity (b) Progressive rainfall suction profile for an Initial phase (c) Progressive rainfall suction profile for 3 Days (d) Progressive rainfall suction profile for 7 Days (e) Progressive rainfall suction profile for 15 Days (f) Progres

Chapter 5: Effect of RPP Spacings on Slope Stability

5.1 Introduction

Shallow slope failures are frequent in embankments constructed on expansive Yazoo clay in Mississippi due to the climatic variation and require significant maintenance budget to repair. Typically, shallow slope failure occurs due to an increase in pore water pressure and reduction of soil strength due to progressive wetting of soil near-surface soil (Khan et al., 2016). This condition further intensified by moisture variation due to seasonal climate change that results in cyclic shrink and swell of the high plastic clay soils. The possible cause of slope failure is defined by penetration of rain water into the cracks, which generate a softened zone in the soil slope (Hossain et al., 2017) Rainfall-induced slope failures are reported to occur during or immediate periods of intense or prolonged heavy rainfall in fine-grained soil (Day et al., 1989; Tohari et al., 2007). During intense or prolonged rainfall period, rain water infiltrates into the slope and creates a temporary perched water condition, which reduces the effective stress on the soil and increases the excess pore water pressure. The combination of the fully softened shear strength and perched water zone due to rainfall mostly cause the shallow slope failure (Khan et al., 2015). Generally, the failure depth is usually within 0.91-1.82 m, and the failure plane remains parallel to the slip surface. The unsaturated state of the soil plays a major role in protecting natural slopes from failure. Slope reinforcement is currently utilized as an effective slope remediation technique for relatively shallow (<5m) slope failure conditions. In situ reinforcement methods for stabilizing slopes and embankments have included soil nailing, drilled piers, micro piles and recycled plastic pins. Recycled Plastic Pins (RPP) had been utilized as a cost-effective solution for slope stabilization compared to conventional techniques (Hossain et al., 2017; Khan et al., 2015; Loehr et al., 2000; Loehr et al., 2007). RPPs are driven into the slope face to provide an additional resistance along the slip plane which restricts the progression of slip surface and increase the factor of safety. RPPs are fabricated from recycled plastics and waste materials (polymers, sawdust, and fly ash) (Chen et al., 2007). It is a lightweight material and less susceptible to chemical and biological degradation compared to other structural materials. The use of RPPS can reduce the waste volume entering landfills and provide additional markets for recycled plastic (Loehr et al., 2000). A typical RPP is composed of High Density Polyethylene, HDPE (55% – 70%), Low Density Polyethylene, LDPE (5% -10%), Polystyrene, PS (2% – 10%), Polypropylene, PP (2% -7%), Polyethylene-terephthalate, PET (1%-5%), and varying amounts of additives i.e. sawdust, fly ash (0%-5%) (McLaren et al., 1995).

Khan et al. (2015) presented a field study over a highway slope located along US 287 near St. Paul overpass in Midlothian, Texas. The slope was constructed using high plastic clay (CH). The surficial movement was observed over the slope which resulted in cracks over the shoulder. As a remediation technique, a total of 3 sections (designated as Reinforced Section 1, Reinforced Section 2 and Reinforced Section 3) were reinforced with RPP. RPP with different spacing (i.e., 0.9 m, 1.52 m and 1.82 m c/c) was utilized in the Reinforced Section 1. On the other hand, Reinforced Section 2 and Reinforced Section 3 were stabilized using uniform 1.21 m c/c spacing. The performance monitoring results of US 287 slope (Figure 5.1) indicated that the settlement at Reinforced Section 1 was 6 cm; whereas, the crest settlements were 12 cm and 8 cm in Reinforced Section 2 and Reinforced Section 3, respectively. The settlement at Reinforced Section 1 was low due to the smaller spacing of RPP (0.9 m) at the crest of the slope. The study summarized that closer spacing of RPP near the crest of the slope, where the tension crack initiates the movement of the slope provide superior performance than the slope stabilized with the uniform spacing of

RPP. During this study, the closer spacing of RPP near the crest and uniform spacing of RPP at the rest of the slope is being utilized.

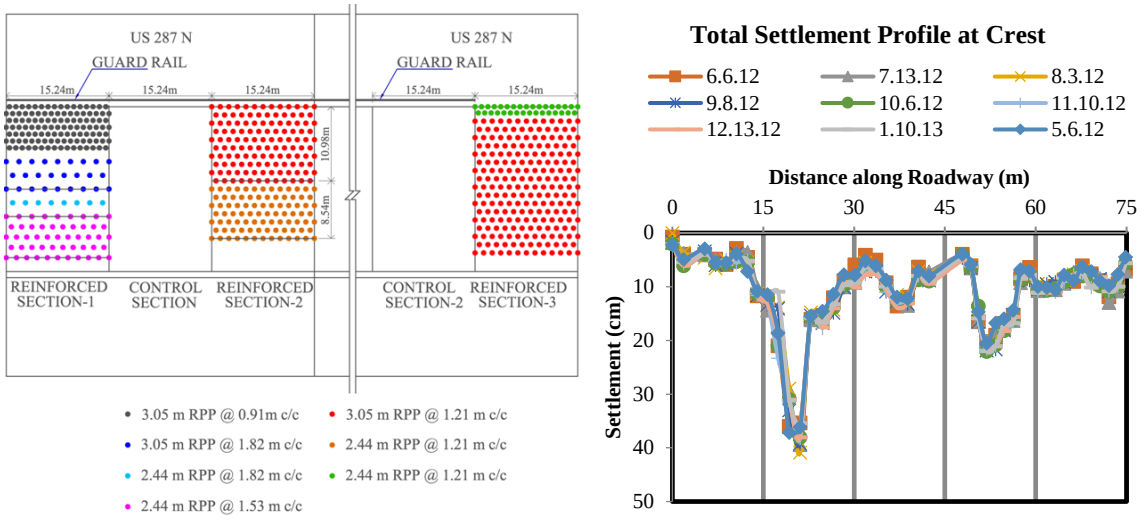

(a) **(b)**

Figure 5.1 Performance of US 287 Slope a. the layout of RPP b. total Settlement profile at the crest of slope (5)

The current chapter summarizes the investigation of the effectiveness of Recycled Plastic Pin in slope on Yazoo clay using Finite element method. A total of three slope sites (2H: 1V, 3H: 1V and 4H: 1V) with uniform spacing of RPP and varied RPP spacing has been utilized. For uniform spacing, 0.91 m c/c., 1.21 m. c/c. and 1.52 m. c/c are selected based on the several field investigations conducted in Missouri, Iowa, and Texas (Hossain et al., 2017). On the other hand, for the varied spacing, each slope is divided into two parts designated as the top part (1/3 length near crest) and bottom part (rest 2/3 length of the slope). The technique includes a constant 0.91 m spacing at the top part near the crest and 1.21 m, 1.52 m and 1.82 m at the rest of the slope. The length of the RPP was 3.04 m. Finite Element Method program PLAXIS has been utilized to investigate the effect of spacing on both safety and deformation of the slope on Yazoo clay.

5.2 Site Condition

During this study, a highway slope located in Jackson Mississippi, which was constructed using marginal Yazoo clay soil and has already shown the surficial movement is selected. Weathered Yazoo clays soil samples from the slope sites are investigated at the laboratory to determine the physical properties such as liquid limit, plasticity index, grain size analysis, and unit weight. The Liquid limit of the Yazoo clay was 108 and Plasticity Index is 84, whereas, the % Passing #200 sieve is more than 94.6%. The unit weight of the soil is considered as 21 kN/m^3 at optimum moisture content using standard Proctor compaction effort. The peak shear strength of the Yazoo clay was determined which indicated that the cohesion and friction angle are 5.22 kPa and 18.7 deg. Khan et al., 2017 investigated the effect of the rainfall on the matric suction and stability of slope constructed on the Yazoo clay soil. The study indicates that the presence of a small variation of matric suction tends to help the slope from failure. On the other hand, continuous rainfall infiltrates through the surface which tends to eliminate the matric suction and forms a temporary perched water condition in the slope. The combination of the fully soften zone and rainfall induce temporary perched

water condition that causes the shallow slope failure in most of the slopes on expansive soil (Khan et al., 2016). The current study includes the effect of the perched water condition along with the fully soften shear strength as a critical condition in FEM analysis, to investigate the slope stabilization scheme using RPP.

5.3 Finite Element Modeling

The Plaxis 2D is a two-dimensional finite element (FE) program used to perform deformation and stability analysis for various types of geotechnical applications (Reference manual, PLAXIS 2D). The elastic-perfectly plastic Mohr-Coulomb soil model was utilized for stability analyses using 15 node-triangular elements. Standard fixities were applied as a boundary condition. The shear strength reduction method (phi-C reduction analysis) was used to determine the factor of safety (FS). The representative highway slope is 9.15 m high with a slope ratio of 3H: 1V. The slope is considered to experience failure with limiting FS to 1.0. The geometry of the slope is developed based on the existing borehole log and soil test results. Moreover, the fully softened shear strength, as determined from the soil test results is utilized at the top soil. Based on the stability analysis result, the factor of safety of the 3:1 slope is observed as 1.27. As a result, the slope is stable and require almost no repair. The additional back analysis is conducted after applying a perched water formation at the top soil layer, considering the effect of rainfall. As a result, the factor of safety of the slope reduces to 1.18. The soil parameters for finite element analysis are summarized in Table 5.1. Three geometries of the slopes with slope ratios of 2H: 1V, 3H: 1V and 4H: 1V is generated, similar to the highway slope in consideration. The geometry of the slopes, as shown in Figure 5.2, are further utilized in finite element analysis. Based on the stability analysis, the factor of safety of the 2H: 1V, 3H: 1V and 4H: 1V slopes are 1.093, 1.277, and 1.62 respectively. The slip surface for each of the slopes (at dry condition) are presented in Figure 5.3. A perched water zone is applied in the top soil layer to simulate the worst-case scenario, as successive rainfall forms the temporary perched water condition that usually causes the shallow slope failure in Mississippi (Khan et al., 2017). The depth of the perched water zone is 7 ft. near the crest. The perched water condition is defined to apply the similar pore water pressure inside the slope. The strength reduction analysis is conducted to evaluate the factor of safety of the slope with the perched water condition. The FEM analysis results indicate that the factor of safety of the 2H: 1V, 3H: 1V and 4H: 1V slope reduced to 0.99, 1.18 and 1.47, respectively when considering the perched water condition (Figure 5.3). This reduced factor of safety is very close to failure for 2H: 1V and 3H: 1V slope. Thus, the unreinforced slope, considering the fully softened shear strength at the top soil with the presence of perched water condition, has been utilized to investigate slope stabilization option using RPP.

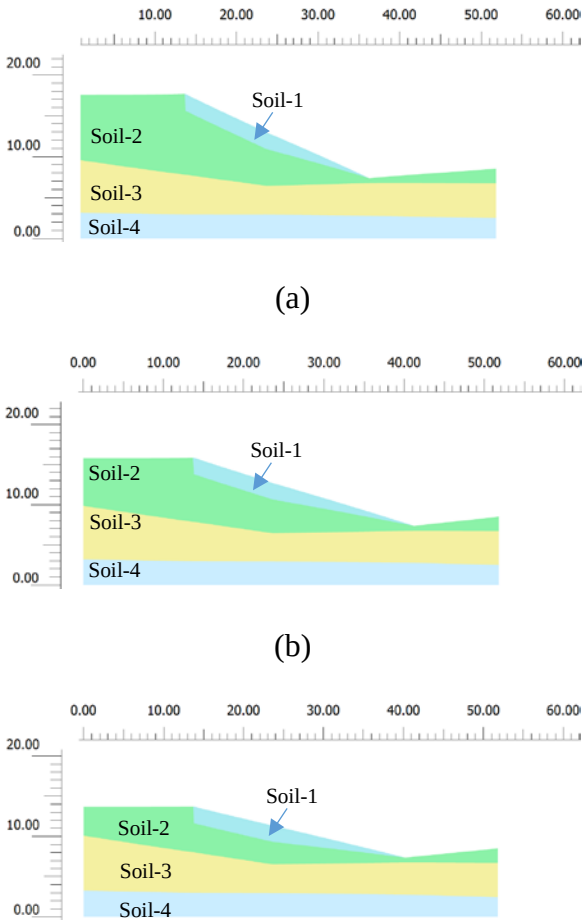

Figure 5.2 Slope Geometries for a. 2H: 1V slope, b. 3H: 1V slope and (c) 4H: 1V slope

Table 5.1 Parameters for FE analysis

Soil Type	**Friction angle φ**	**Cohesion c**	**Unit Weight γ**	**Elastic Modulus E**	**Poisson Ratio ν**	**RPP Parameters**		
-	◦	kN/m^2	kN/m^3	kN/m^2	-			
1	18	5.221	21	4788	0.35	EA	kN/m	21.4E3
2	23	23.94	21	7183	0.30	EI	kN m^2/m	1.310E6
3	25	47.89	22	9576	0.25	d	m	27.1
4	35	143.64	22	11970	0.2			

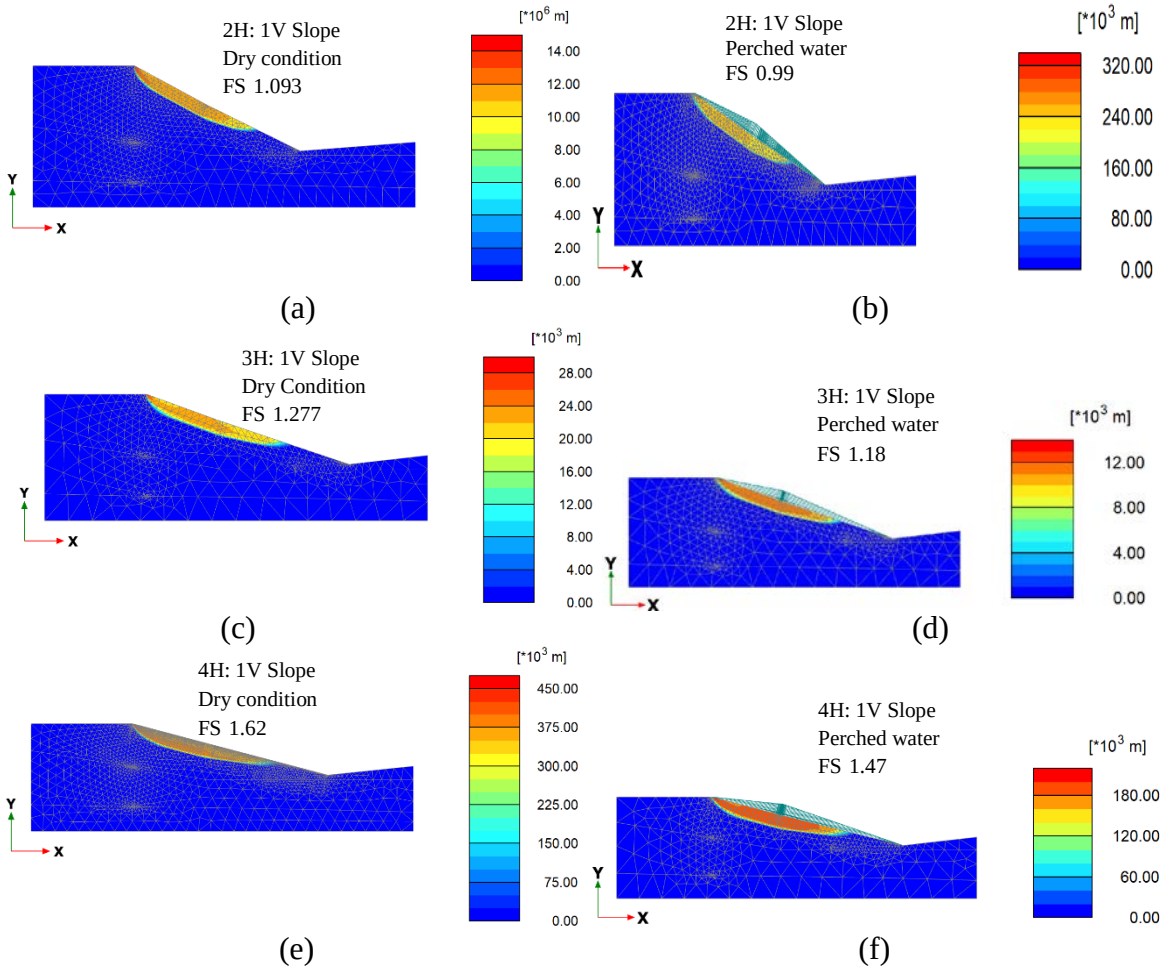

Figure 5.3 Stability Analysis of the unreinforced slope (a) 2H: 1V slope (dry condition) (b) 2H: 1V slope (perched water condition), (c) 3H: 1V slope (dry condition), (d) 3H: 1V slope (perched water condition), (e) 4H: 1V slope (dry condition), (f) 4H: 1V slope (p

5.4 RPP Configuration for Slope Stabilization Option

The current study investigates the performance and safety of reinforced slope on Yazoo clay using RPP. As a part of the study, each slope ratio is divided into two parts designated as the top part (1/3 length near crest) and bottom part (rest 2/3 length of the slope). The top part of each slope ratio is reinforced with 0.91 m RPP spacing to provide additional resistance against deformation while the rest of the slope is considered with a higher spacing of RPP. The RPP is modeled as the plate element. The properties of RPP are also summarized in Table 5.1. A total of six different RPP spacing are considered for each slope ratio which is designated as configuration A, B, C, D, E and F. RPP configuration A, B and C are modeled with uniform RPP spacing of 0.91 m, 1.21 m and 1.52 m, respectively. On the other hand, different RPP spacing is utilized in configurations D, E and F, where at the top part RPPs are kept in constant spacing 0.91 m, and 1.21 m, 1.52 m and 1.82 m RPP spacing is considered at the bottom part of each slope. The details of the study are summarized in Table 5.2 and Figure 5.4.

Table 5.2 Numerical Modeling Matrix

Slope Ratio	RPP Configuration	RPP Spacing all length of Slope	RPP Spacing at 1/3 length of Slope near Crest (Top Part)	RPP Spacing at 2/3 length of Slope near Crest (Bottom Part)
2H:1V, 3H:1V and 4H:1V	A	0.91 m	-	-
	B	1.22 m	-	-
	C	1.52 m	-	-
	D	-	0.91 m	1.22 m
	E	-	0.91 m	1.52 m
	F	-	0.91 m	1.83 m

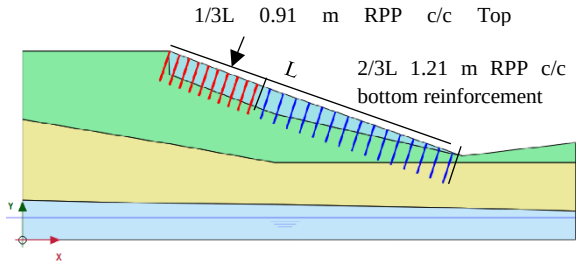

(a)

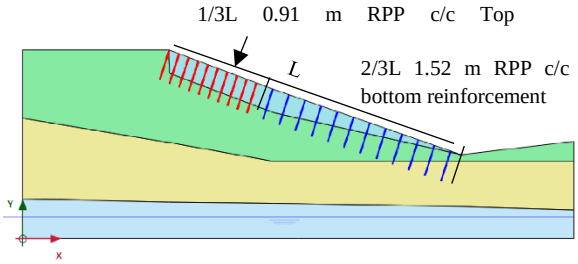

(b)

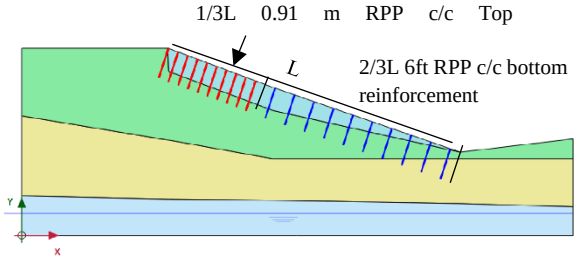

(c)

Figure 5.4 RPP Layout at top and bottom part of slope (a) Configuration D (b) Configuration E and (c) Configuration F

5.5 Slope Stability Analysis of the Reinforced Slope

The factor of safety of the reinforced slope is calculated using the strength reduction technique. Based on the FEM analysis the variation of a factor of safety with various RPP spacing is presented in Figure 5.5, Figure 5.6 and Figure 5.7. The factor of safety of the each RPP configuration is summarized in Table 5.3. Based on the FEM analysis results, the 0.91 m spacing (configuration A) provides the highest

factor of safety of the 2H: 1V slope. The factor of safety of the unreinforced 2H: 1V slope is 0.99, whereas including the 3.04 m long RPP which are placed at 0.91 m c/c increase the factor of safety to 1.73. Moreover, the factor of safety with 1.21 m spacing (Configuration B) is close to the factor of safety of 0.91 m spacing. With 1.52 m. spacing (Configuration C), a slight drop in the factor of safety is observed, with a value of 1.68. The factor of safety of the Configuration D (0.91 m spacing near crest and 1.21 m. spacing near the toe) has the same value of the factor of safety as Configuration C. The factor of safety of the Configuration E (0.91 m spacing near top and 1.52 m. spacing near the toe) and Configuration F (0.91 m spacing near top and 1.82 m spacing near toe) has a factor of safety of 1.64 and 1.62, respectively. The increment of the factor of safety of the 3H: 1V and 4H: 1V has followed the similar trend with different RPP configuration, as the 2H: 1V slope. Based on Figure 5.6 and Figure 5.7, the factor of safety of the slope increases to 2.12 and 2.64 for the 3H: 1V and 4H: 1V slope with 0.91 m spacing all over the slope. On the other hand, the lowest factor of safety of the reinforced 3H: 1V and 4H: 1V slope is observed as 2.08 and 2.18 respectively, with RPP configuration F (0.91 m spacing near crest and 1.82 m spacing near the toe of the slope). As presented in Table 5.3, with the perched water condition in the fully soften the soil, the 2H: 1V and 3H: 1V has a marginal factor of safety of 0.99 and 1.18, respectively. With the inclusion of the RPP at different configuration, the factor of safety of the reinforced slope increase to a range in between 1.62 and 2.08, which is higher than 1.5 which is required by several state and federal agencies for slope repair. Therefore, in terms of safety, all the RPP configuration provide enough support to make the reinforced slope stable.

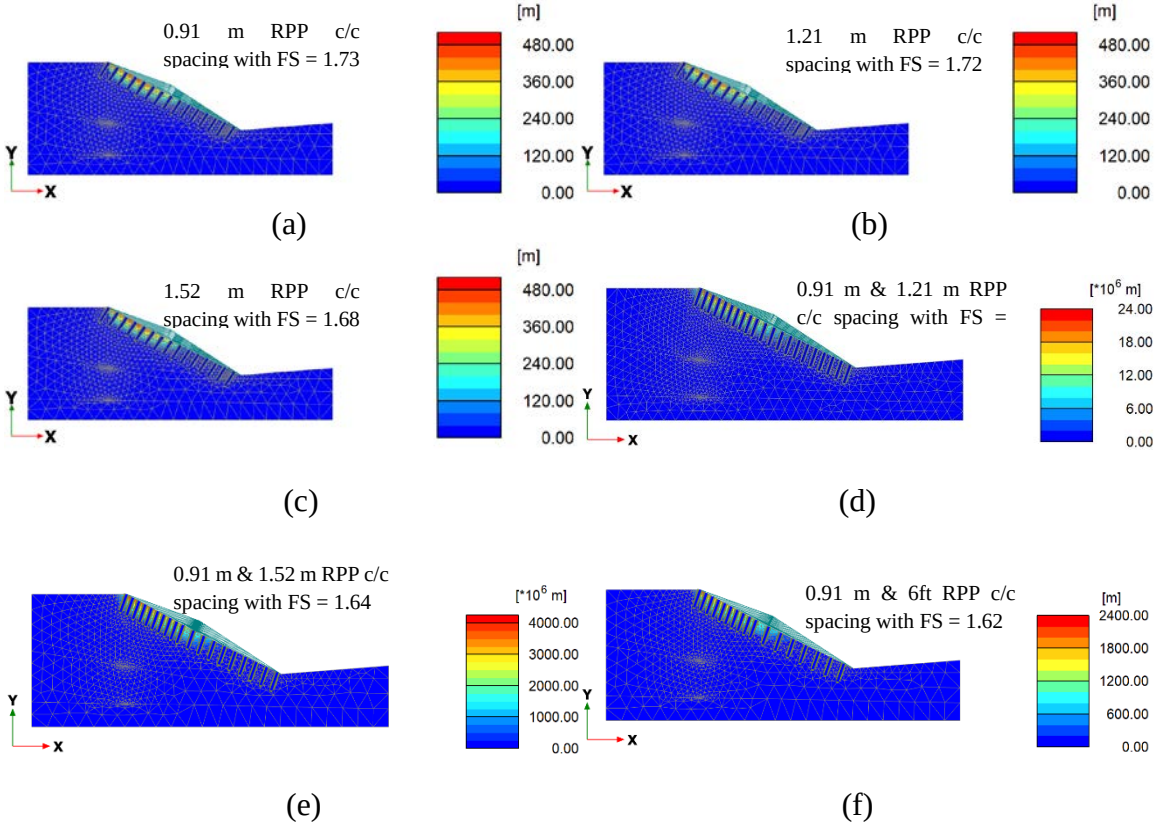

Figure 5.5 Stability analysis results in 2H: 1VSlope with different RPP Spacing (c) 1.52 m RPP Spacing (d) 0.91 m & 1.21 m RPP Spacing (e) 0.91 m & 1.52 m RPP Spacing (f) 0.91 m & 6ft RPP Spacing

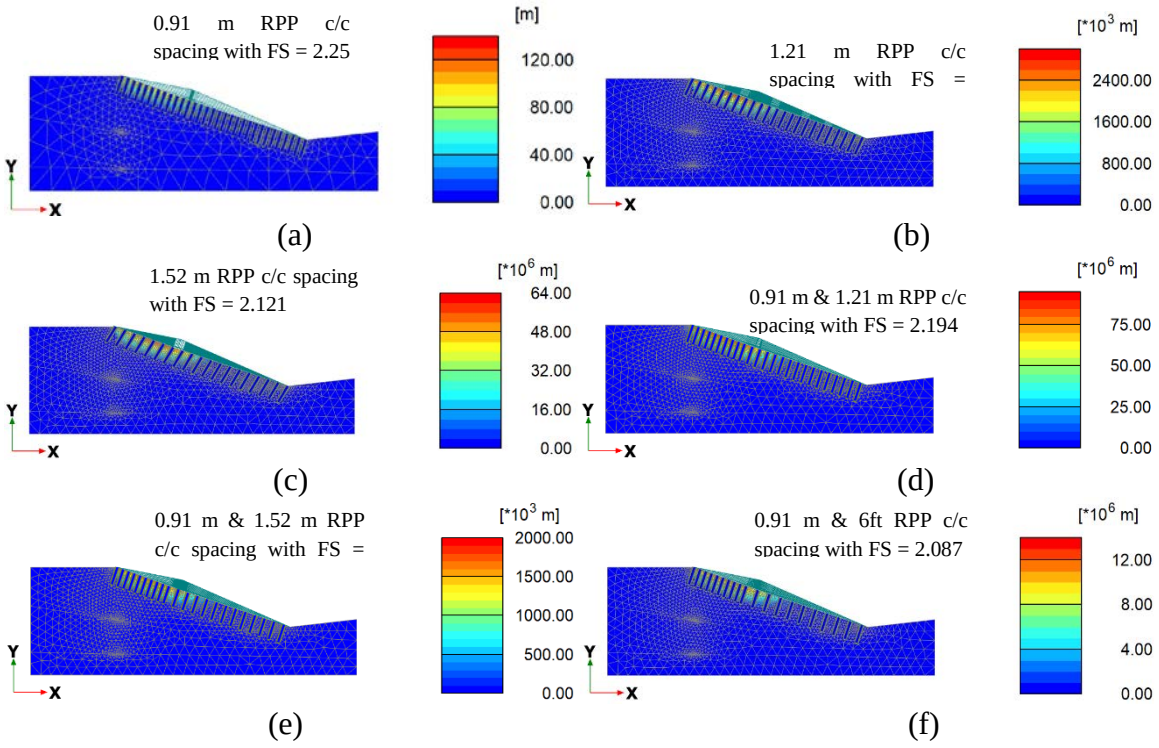

Figure 5.6 Stability analysis results in 3H: 1V Slope (a) 0.91 m RPP Spacing (b) 1.21 m RPP spacing (c) 1.52 m RPP Spacing (d) 0.91 m & 1.21 m RPP Spacing (e) 0.91 m & 1.52 m RPP spacing (f) 0.91 m & 6ft Spacing

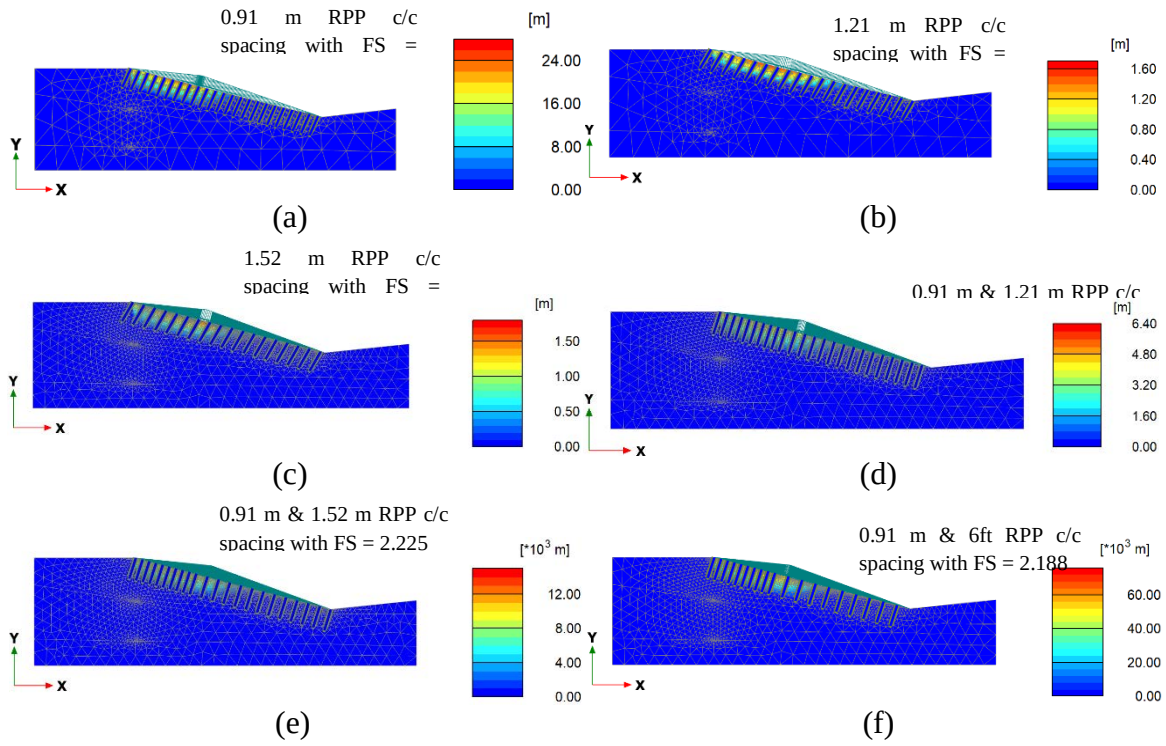

Figure 5.7 Stability Analysis results in 4H:1V Slope (a) 0.91 m RPP Spacing (b) 1.21 m RPP Spacing (c) 1.52 m RPP Spacing (d) 0.91 m & 1.21 m RPP Spacing (e) 0.91 m & 1.52 m RPP Spacing (f) 0.91 m & 6ft RPP Spacing

Table 5.3 FS values for different RPP Spacing in 2:1, 3:1 and 4:1 Slopes

Slope Ratio	Initial factor of safety	RPP Configuration					
		A	**B**	**C**	**D**	**E**	**F**
		0.91 m RPP Spacing	***1.21 m RPP Spacing***	***1.52 m RPP Spacing***	***0.91 m &1.21 m RPP spacing***	***0.91 m and 1.52 m RPP Spacing***	***0.91 m and 6ft RPP spacing***
2H:1V Slope	0.99	1.73	1.72	1.68	1.68	1.64	1.62
3H:1V Slope	1.18	2.25	2.18	2.12	2.19	2.11	2.08
4H:1V Slope	1.47	2.76	2.72	2.65	2.48	2.22	2.18

5.6 Deformation at the Crest

The plastic calculation is performed in Plaxis for deformation analysis. An initial condition of the slope is generated using gravity loading condition which is recommended for non-level ground such as slope. During gravity turn-on analysis, the vertical stress is calculated based on the weight of unstressed mesh, and then horizontal stresses are changed to be equal to k0 (earth pressure coefficient at rest) times the calculated vertical stress. Later, the plastic analysis was conducted by activating the RPP in the soil

model. Based on the FEM analysis, the maximum lateral deformation of 3.04 m long RPP at the crest of the slope with different RPP configuration at top section is presented in Figure 5.8. The horizontal displacement plots presented that, the RPP has rotational movement. In addition, the RPP experience a translational movement near the base, which implied that it is not fixed at the base. As a result, the movement of the RPP is similar to the movement of the short pile, which does not have enough fixities in the slope. It should be noted that the depth of soft soil in the FEM analysis is 2.13 m. As a result, the 3.04 m long RPP has only 1/3 of its length into the stiffer base. However, deformation of the slope is negligible. During this study, only the deformation of slope at the crest (from top section) is presented. The deformation of the bottom section (at middle and toe) of the slope is observed less compared to the displacement at the crest. Therefore, no deformation result from the bottom section of the slope is presented here. Based on the plastic analysis results, the uniform 0.91 m (configuration A), 1.21 m. (configuration B) and 1.52 m. (configuration C) the spacing of RPP provides enough resistance at the crest of the 2H: 1V slope. As a result, the horizontal movement of the RPP is overserved within a range of 12 mm. However, for the varied spacing of RPP, 0.91 m/1.21 m (configuration D), 0.91 m/1.52 m. (configuration E) and 0.91 m/1.82 m (configuration F) has significant high deformations at the top of the RPPs within a range of 225 mm or greater. It should be noted that the configuration D, E, and F has a high factor of safety within a range of 1.62 and 1.68. However, they have significant high movement. Therefore, the configuration D, E, and F are not recommended in the 2H: 1V slope. The uniform RPP spacing of 0.91 m (configuration A), 1.21 m. (configuration B) and 1.52 m (configuration C) and different spacing of 0.91 m/1.21 m (configuration D), 0.91 m/1.52 m (configuration E) and 0.91 m/1.82 m (configuration F) has a similar movement trend at the crest of the 3H: 1V and 4H: 1V slope. Based on Figure 5.8, the maximum horizontal displacement at the RPP top was observed as 7 mm, which is almost negligible. In addition, all the configuration has a high factor of safety with 3H: 1V and 4H: 1V slope. Since the varied spacing with 0.91 m at the top part and 1.21 m. to 1.82 m at the bottom part require less RPP to reinforce the slope, the cost of the slope repair will be less. Therefore, the configuration D, E, and F are recommended for 3H: 1V and 4H: 1V slope.

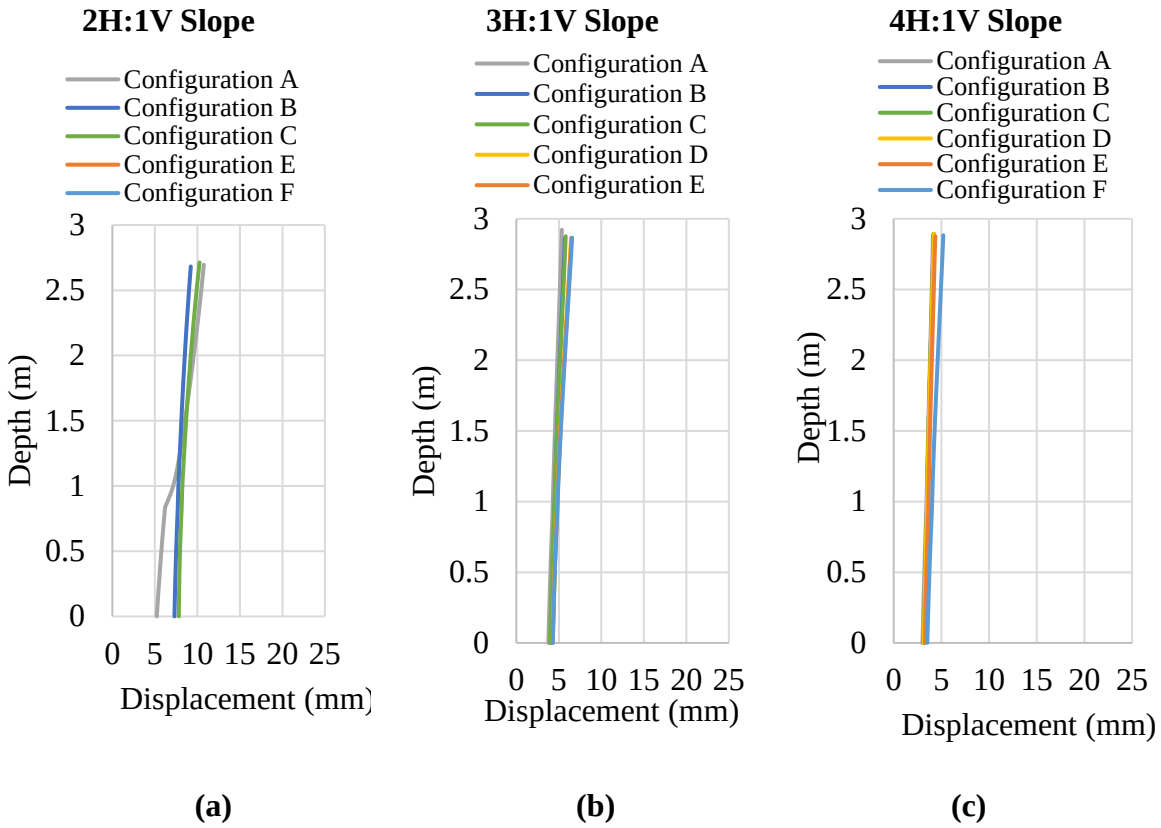

(a) **(b)** **(c)**

Figure 5.8 Horizontal Displacement Profile of RPP at a. 2H:1V slope, b. 3H: 1V slope and c. 4H: 1V slope

Chapter 6: Design Procedures

6.1 Introduction

Recycled Plastic Pin (RPP) has been utilized as a sustainable and cost-effective measure for stabilizing shallow slope failures in Texas, Missouri, and Iowa (Hossain et al., 2017; Khan et al., 2015; Khan et al., 2013; Loehr et al., 2007). It is a lightweight material and is less susceptible to chemical and biological degradation, is resistant to moisture, and requires almost no maintenance, thus making it a more attractive alternative than other structural materials (Loehr et al., 2007). Moreover, the use of plastic pin reduces the volume of waste entering the landfill and provides an additional market for recycled plastic. RPPs are predominantly a polymeric material, fabricated from recycled plastics and other waste materials (Chen et al., 2007; Malcolm et al., 1995; Lampo et al., 1997; McLaren et al., 1999; Khan et al., 2013). RPPs are installed on the slopes to intercept potential sliding surfaces, which provides additional resistance and helps to maintain the long-term stability of the slope. Loehr and Bowders, 2007 referred to the resistance of RPP as the limit resistance, which varies along the depth of the RPP. The author considered two soil failure mechanisms and two structural failure modes and established a limit resistance curve for RPP (Bowders et al., 2003; Loehr et al., 2007). The design approach considered by Loehr and Bowders, 2007 was simple and very straightforward. However, while it considered the structural failure modes of RPP, it did not explain the deformation of the reinforced slope. Chen et al., 2007 performed a study on the creep behavior of RPP. They concluded that due to the variety of manufacturing processes and constituents, the engineering properties of commercially available materials vary substantially. The polymeric materials are durable in terms of environmental degradation, but they can exhibit higher creep rates than other structural materials such as timber, concrete, or steel. It is important to consider the creep criteria in the design of a RPP-stabilized slope. The use of RPP for routine maintenance in stabilizing shallow slope failures is under serious consideration due to the environmental benefits and cost effectiveness it affords. Yet, the lack of the existence of any simple design approach is a major constraint.

The current chapter presents the development of a design approach for stabilizing slopes using RPP. The limit resistance of RPP is evaluated as to its ability to control the performance of the reinforced slope. Since the modulus of elasticity of RPP is low (690 MPa to 3100 MPa, (Breslin et al., 1998)) compared to other structural materials, it is important to consider the anticipated displacement due to the applied soil pressure. The creep criteria should also be considered for the limit resistance of RPP. Therefore, two limiting criteria of RPP have been taken into account in developing the design approach: limit horizontal displacement of RPP and limit maximum flexure of RPP to resist creep failure. A robust numerical analysis was conducted using the finite element modeling (FEM) software Plaxis to develop design charts for limiting the horizontal displacement and creep failure of RPP. The FEM analysis was conducted for different slope angles (2H: 1V to 4H: 1V), soil strengths (c = 4.75 kPa, $\Phi = 0^o$ to c = 23.9 kPa, $\Phi = 30^o$), and depths of slip surfaces (0.9 m to 2.13 m). After the development of the design charts, the design approach was validated against the factor of safety determined by using the FEM analysis of two highway slopes. The development of the limiting criteria and design approaches are presented in the following sections.

6.2 Limitation Criteria

6.2.1 Criteria to Limit Horizontal Displacement of RPP

RPP is subjected to active pressure and passive resistance of soil when it is installed as slope reinforcement. In addition, due to the sliding of the slope, RPP is subjected to an additional soil pressure above the slip surface. The schematic of the load over the RPP is also illustrated in Figure 6.1. RPPs get Anchorage from the foundation soil below the slipping plane, work as a lateral support, and resist the movement of soil above the slip surface. However, during this interaction, a displacement takes place, which depends on the additional pressure due to slope movement, the depth of the soft soil over the slipping plane, the active and passive pressure of the soil, and the anchorage from the foundation. Based on the displacement of RPP during this interaction, the overall displacement of the slope should take place. It is important to limit the displacement of the RPP as slope reinforcement in order to limit the overall displacement of the slope. Therefore, the current study considered the limit horizontal displacement approach where the capacity of RPP was evaluated based on the anticipated displacement due to the soil movement.

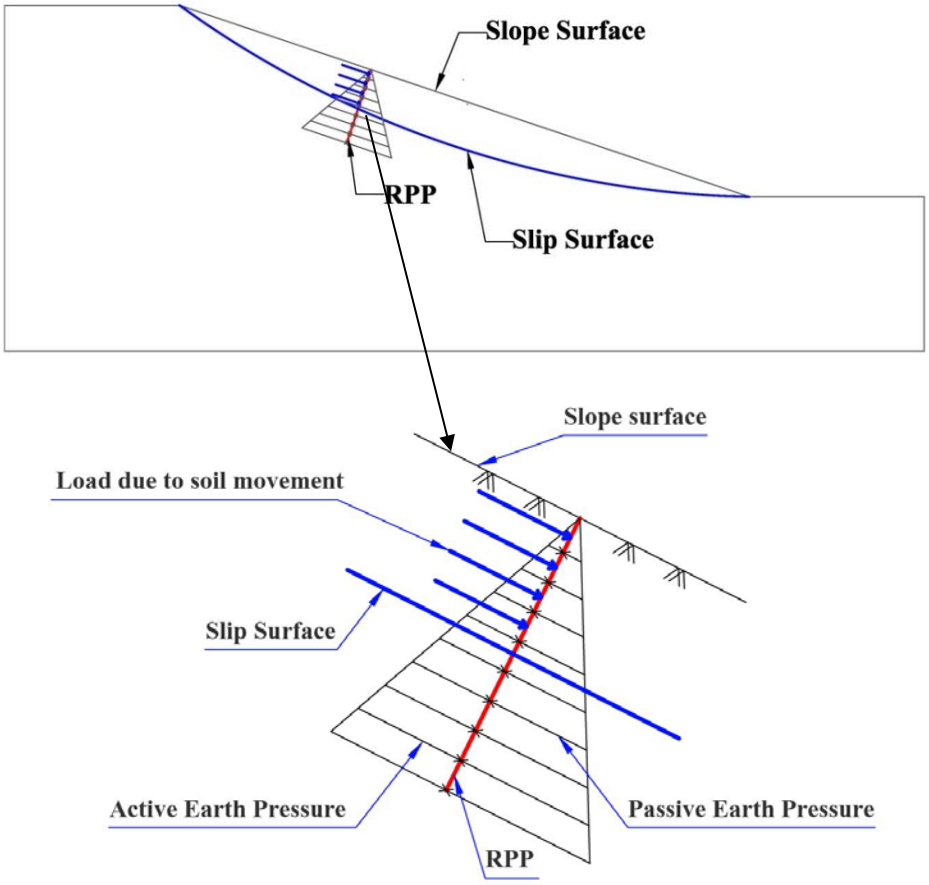

Figure 6.1 Schematic of load over RPP as slope reinforcement

6.2.2 Criteria to Limit Maximum Flexure for Prolonged Creep Life

Chen et al., 2007 presented a study on the creep behavior of RPP. The author studied the flexural creep responses on scaled RPP samples at different temperatures, such as 21°, 35°, 56°, 68°, and 80°C. The study considered the Arrhenius method to estimate the long-term creep behavior. Based on the study, Chen et al., 2007 observed that as the temperature increased, the time to reach failure decreased for the same load condition. In addition, the loading levels, along with temperature, affected the creep behavior of the recycled plastic specimens. The study presented that at higher load levels, close to the ultimate strength of the material, the creep rate was faster, and it required a shorter time to reach failure. Chen et al., 2007 presented a method to determine the design life of RPP based on a percentage of load mobilization, which indicated that at the higher mobilized loads, the design life of RPP became susceptible to creep failure. Additionally, limiting the percentage of flexural stress in RPP increased the time to creep failure. The study performed by Chen et al., 2007 indicated that at 35% of flexural stress, the estimated time to flexure-creep failure should be 100 years, which is higher than the average design life of a highway slope. Therefore, in this study, an RPP was restricted to 35% of flexural stress to its ultimate capacity.

6.3 Development of Design Chart

The design chart has developed a determination of horizontal deformation and flexural stress by applying external lateral pressure on RPP, using the Finite Element Method. The flow chart for the development of the design chart is illustrated in Figure 6.2. The details are presented in the subsequent section.

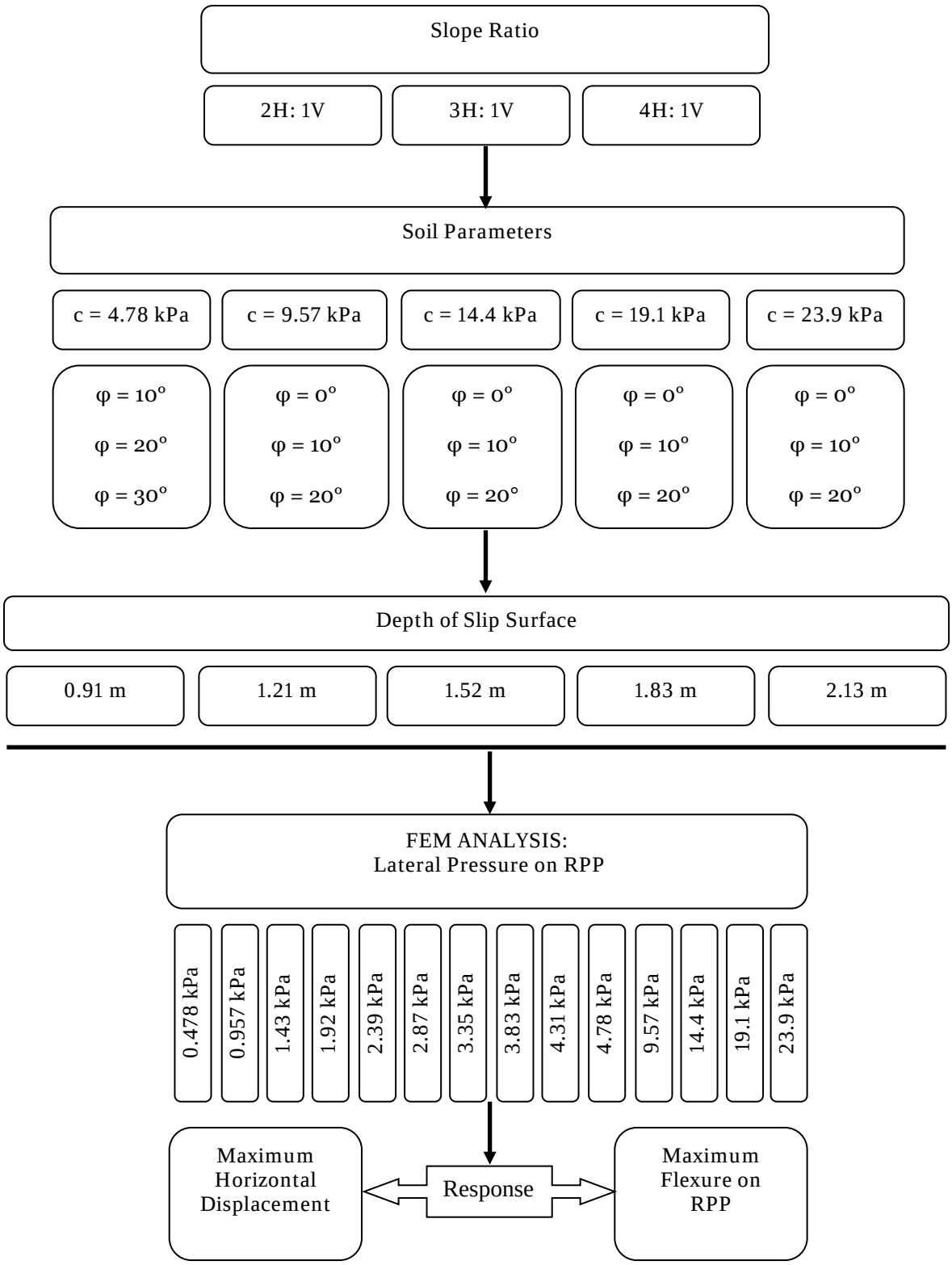

Figure 6.2 Flow Chart for Development of Design Charts

Based on the FEM analysis, during this study, the composite limit resistance curve was developed for different slope ratios and strength parameters. The developed limit resistance curves were utilized and are presented later in this paper.

6.4 Determination of Limit Horizontal Displacement and Maximum Flexure of RPP

The elastoplastic finite element method (FEM) is an accurate, robust, and simple method. This technique was utilized to evaluate the stability of slopes reinforced with piles or anchors under a general frame, where soil-structure interactions are considered, using a zero-thickness elastoplastic interface element. A numerical study was conducted to design the slope stabilization, using recycled plastic pins (Khan et al., 2014; Khan et al., 2013; Hossain et al., 2012), and the finite element method was utilized to evaluate the resistance of RPP. The deformation analysis was performed using PLAXIS 2D. The 8.9 cm x 8.9 cm square-shaped RPP, which is commercially available, was considered as an elastic material (Elasticity Modulus = 200 MPa) and modeled as a plate element. The elastic-perfectly plastic Mohr-Coulomb soil model was utilized for stability analysis, using 15-node triangular elements. The 15-node elements provided a fourth order interpolation for displacements and numerical integration that involved twelve stress points. The 15-node triangle element is very accurate and historically has produced high-quality stress results for different problems (Reference manual, Plaxis 2D). Standard fixities were applied as boundary conditions, where the two vertical boundaries were free to move vertically and were considered fixed in the horizontal direction. The bottom boundary was modeled as a fixed boundary. The FEM analysis was performed using the soil properties as presented in Table 6.1. It should be noted that two layers of soil were considered in the soil model. They were designated as top soil and foundation soil, and are presented in Figure 6.3. During this analysis, the depth of the slipping surface varied between 0.91 m and 2.13 m, with different slope ratios: 2H: 1V to 4H: 1V. The top layer above the slipping surface varied during the analysis (c = 4.75 kPa to 23.9 kPa and $\Phi = 0^{o}$ to 30^{o}), as summarized in Figure 6.2. On the other hand, the bottom layer was considered stiff foundation soil. The deformation analysis was conducted by applying uniform pressure (0.478 kPa to 23.9 kPa) over the RPP throughout the sliding depth and the corresponding maximum horizontal deformation. The maximum bending moment was determined, as presented in Figure 6.3. The value of limit resistance of RPP was determined by integrating the pressure along the depth.

Table 6.1 Parameters for FE analysis

Soil Type -	Friction angle φ ◦	Cohesion c kPa	Unit Weight γ Kg/m^3	Elastic Modulus E kPa	Poisson Ratio ν -	RPP properties	Unit	Parameters
Top Soil	10	9.57	2000	96.95	0.35	EA	kN/m	16678
						EI	kNm^2/m	10.98
Foundation Soil	30	23.9	2000	1778.3	0.30	d	m	0.088

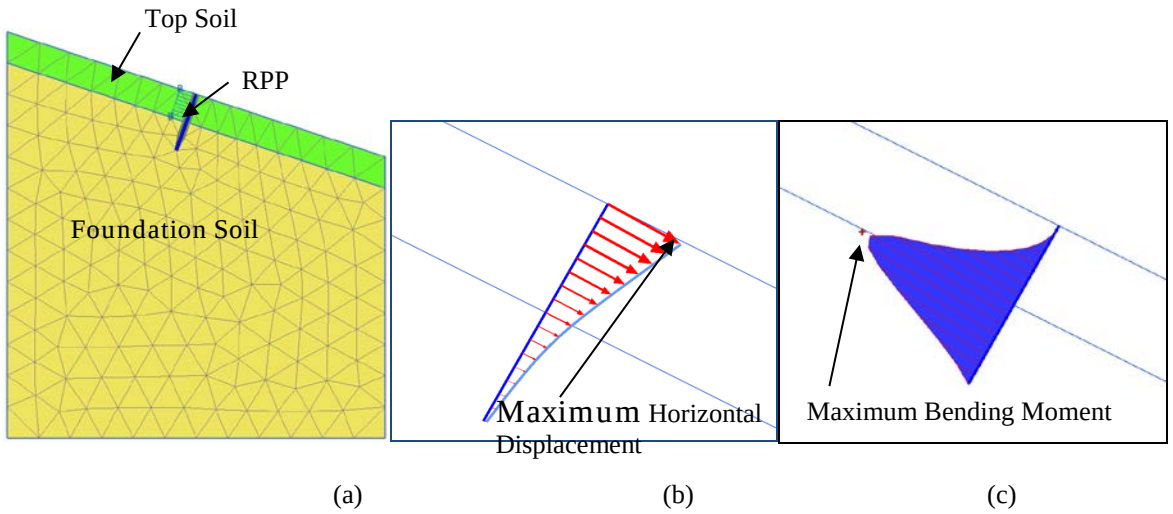

Figure 6.3 Determination of Response of RPP due to Applied Load, a. Maximum Horizontal Displacement, b. Maximum Bending Moment

The total resistance of RPP (designated as limit resistance) with corresponding horizontal deformation and maximum flexure stress is summarized for a given soil strength of top soil with a varied depth of slip surface, as presented in Figure 6.4. For example, cohesion c = 9.57 kPa and friction angle ϕ =10˚. Detailed parameters for the FEM analysis are shown in Table 6.1.

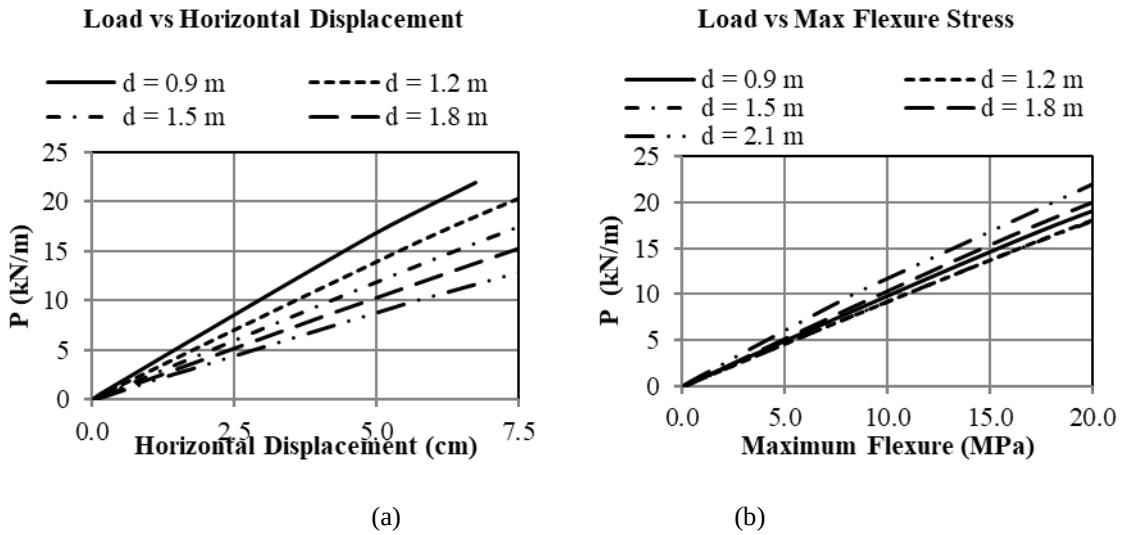

Figure 6.4 Limit Resistance Curve for RPP for c = 9.57 kPa and ϕ = 10˚, a. Load vs. Horizontal Displacement for Slope 3H:1V, b. Load vs. Maximum Flexure for Slope 3H:1

6.5 Finalizing Design Chart

A series of design charts (limit soil failure, limit horizontal displacement, and limit maximum flexure) was developed, similar to Figure 6.4, based on different soil strength parameters and slope ratios, as presented in Figure 6.2. The details of the study are presented in Khan, 2013. Based on the developed charts, the lowest limit resistance of the two limit resistances should be used in the design. The lowest limit

resistance of RPP was determined from different design charts at each soil condition and slope ratio, with allowable horizontal displacement up to 5 cm and flexural stress of 3.4 kPa. It was interesting to observe that the lowest limit resistance of RPP was similar for different soil strengths. Therefore, based on the limit resistance of the RPP, the design charts for various soil strengths were grouped into four soil types. The grouped soil types are presented in Table 6.2. The combined design charts for each soil type are shown in figure 6.5. Table 6.2 and Figure 6.5can be used together to determine the limit resistance of RPP to calculate the factor of safety of a RPP-reinforced slope.

Table 6.2 Soil Groups for the Design Charts

Friction Angle	**Cohesion (kPa)**				
	4.78	**9.57**	**14.4**	**19.1**	**23.9**
0		Soil Group 1	Soil Group 2	Soil Group 2	Soil Group 3
10	Soil Group 1	Soil Group 2	Soil Group 2	Soil Group 3	Soil Group 3
20	Soil Group 2	Soil Group 2	Soil Group 3	Soil Group 4	Soil Group 4
30	Soil Group 2	Soil Group 3	Soil Group 3	Soil Group 4	Soil Group 4

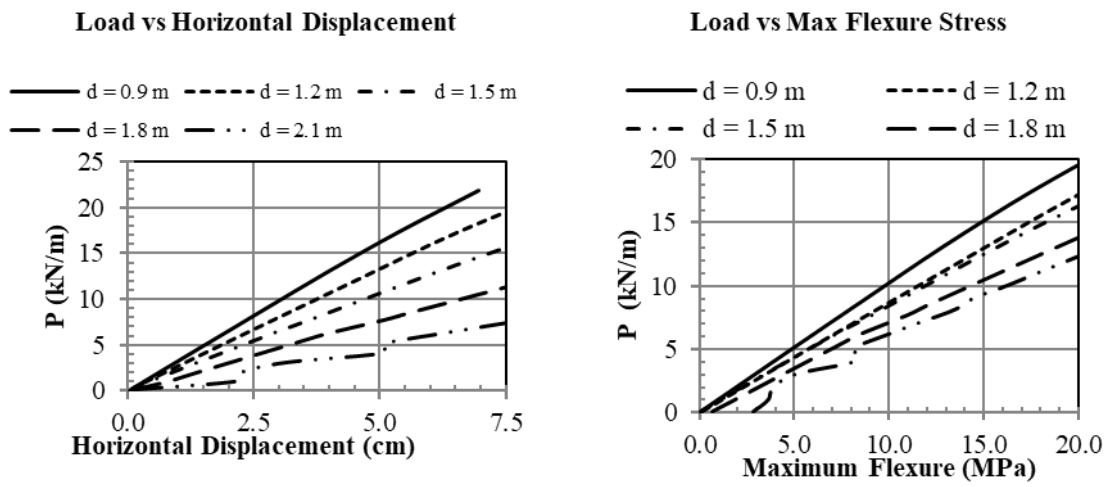
Load vs Horizontal Displacement
d = 0.9 m
d = 1.2 m
d = 1.5 m
d = 1.8 m
d = 2.1 m
P (kN/m)
Horizontal Displacement (cm)
Load vs Max Flexure Stress
Maximum Flexure (MPa)

(a)

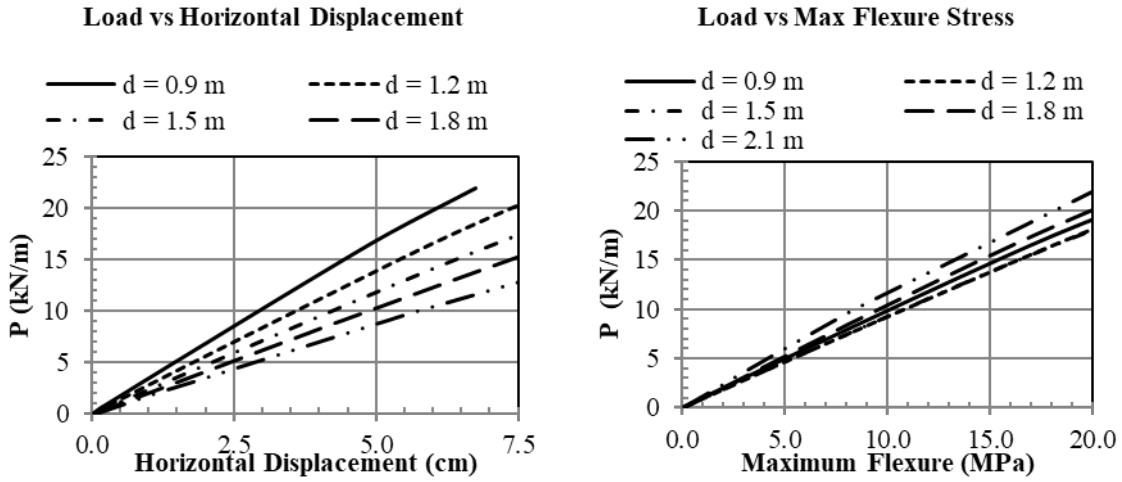
Load vs Horizontal Displacement
d = 0.9 m
d = 1.2 m
d = 1.5 m
d = 1.8 m
P (kN/m)
Horizontal Displacement (cm)
Load vs Max Flexure Stress
d = 2.1 m
Maximum Flexure (MPa)

(b)

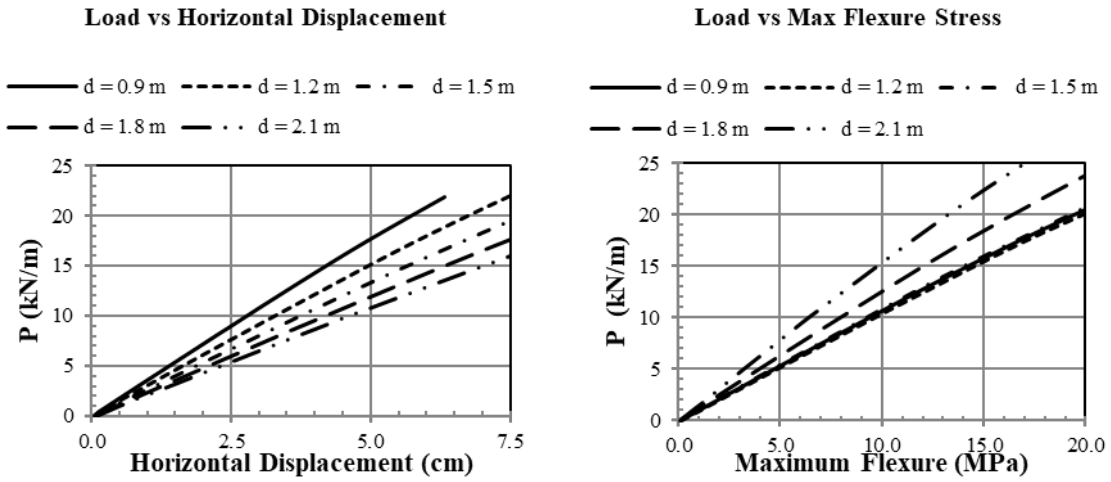

(c)

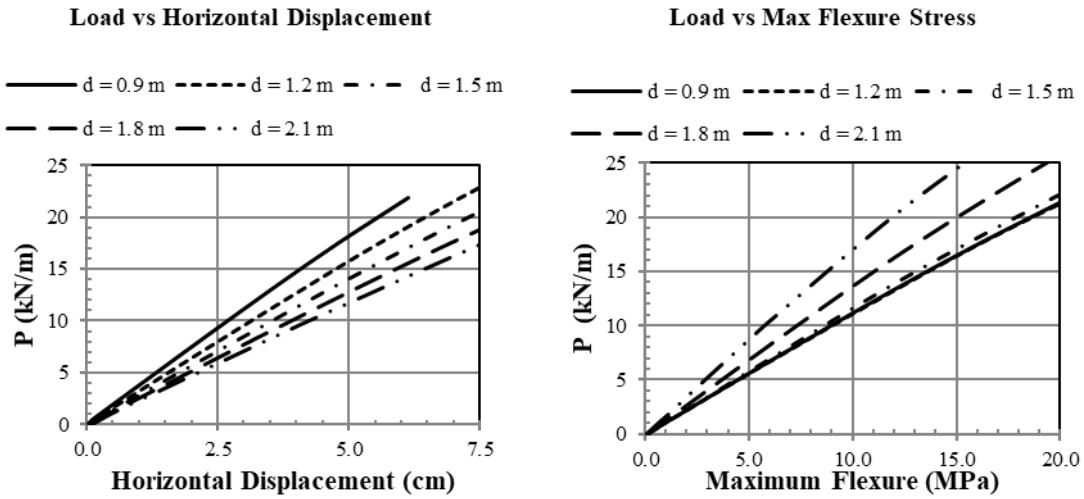

(d)

Figure 6.5 Design Chart (a) Soil Group 1, (b) Soil Group 2, (c) Soil Group 3 and (d) Soil Group 4

6.6 Calculation of Factor of Safety

The limit resistance of RPP can be determined from the design charts and can be utilized as pile resistance in most of the commercial slope stability analysis software to determine the factor of safety of the reinforced slope. Moreover, the design charts can be used, and slope stability analysis can be performed using hand calculation by infinite slope approach. The schematics of the infinite slope approach of the reinforced slope using RPP are illustrated in Figure 6.6.

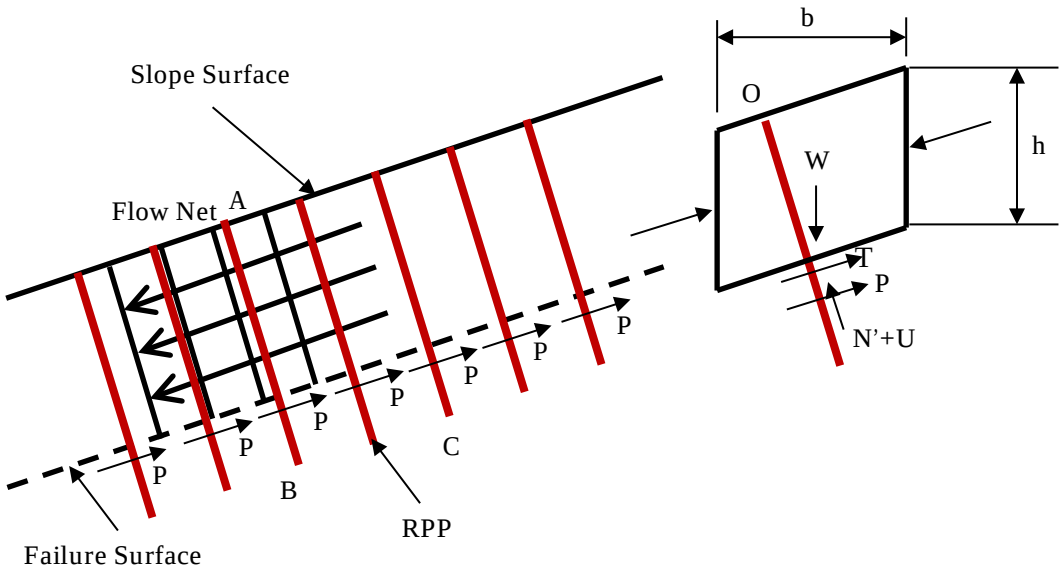

Figure 6.6 **Schematic of Infinite Slope Approach for Reinforced Slope**

6.7 Infinite Slope Approach

The factor of safety of the surficial failure can also be conducted using the infinite slope approach, with seepage parallel to the slope face. Considering the seepage through the soil and water level coinciding with the ground surface, the factor of safety of the unreinforced slope is defined as,

$$FS = \frac{c' + h\,\gamma' cos^2\beta * tan\varphi'}{\gamma_{sat} * h * sin\beta * cos\beta} \qquad (3)$$

The RPP provides additional resistance P in the reinforced slope along the base, as presented in Figure 6.6, and increases the shear resistance. Therefore, the factor of safety equation for the reinforced slope can be determined as,

$$FS = \frac{c'L + hL\,\gamma' cos^2\beta * tan\varphi' + \left(\frac{L}{S} + 1\right) * P}{\gamma_{sat} * hL * sin\beta * cos\beta} \qquad (4)$$

Where,

L = Length (parallel to slope face)

S = RPP spacing

P = Lowest limit resistance of RPP

The composite curve, as presented in Figure 6.5, can be utilized to determine the lowest limit resistance (P) of RPP.

6.8 Design Steps using Infinite Slope Approach

The Infinite Slope is the simplest approach to determining the factor of safety of both unreinforced and reinforced slopes, and it can be performed by using a simple excel spreadsheet. The design can be executed with the following steps:

- The factor of safety of the unreinforced slope should be determined by using the soil parameters and depth of surficial failure, according to the Equation 3.
- The lowest limit resistance 'P' should be determined from the design chart presented in Figure 6.5, by using the depth of failure.
- The spacing of RPP should be considered.
- Finally, the factor of safety of the reinforced slope can be determined by using Equation 4.
- If the factor of safety of a reinforced slope is inadequate, the spacing of the RPP should be reduced to increase the factor of safety of the reinforced slope.

Chapter 7: Conclusion

7.1 Conclusion and Final Recommendation

Multimodal transportation systems (MTS) facilitate efficient movement of people, goods, and services, and are critical national infrastructure components to maintain the nation's economic health. MTS is highly interconnected with numerous other infrastructure systems, which includes communications, emergency response, energy, water supply, agricultural production, and manufacturing. A lack of performance from any one system can have substantial detrimental effects on the performance of the interrelated systems.

Slopes and embankments are integral component of the maritime and multimodal transportation system. Shallow failure often cause significant hazards to multimodal transportation infrastructure and if not properly maintained, it requires more extensive and expensive repairs (Loehr and Bowders, 2007; Loehr et al., 2007). Many of the slopes in multimodal transportation infrastructure of Mississippi are constructed using marginal highly plastic clay soil (Yazoo clay) which are expansive in nature and are known to be susceptible to shallow landslide. Typically, shallow slope failure occurs due to an increase in pore water pressure and reduction of soil strength due to progressive wetting of soil near-surface soil. This condition is further intensified by moisture variations due to seasonal climatic changes that results in cyclic shrink and swell of the high plastic clay soils.

The Recycled Plastic Pin (RPP) can be an attractive choice to stabilize the shallow slope failure in Mississippi. The current study investigated the effect of rainfall on the slope failure, numerically investigates different RPP configuration at 2H: 1V, 3H: 1V and 4H: 1V slopes and developed a design protocal to stabilize Mississippi slopes using RPP. Based on the study, it can be concluded that:

- Based on the flow analysis results, it was observed that there is a high suction at the initial moment before rainfall. With short duration of rainfall, a decrease in the suction takes place. This decrease in suction is immediate at the shallow surface faster compared to the deeper surface. It was also noticed that with an increase of rainfall intensity does not affect much infiltration, due to the low permeability of the highly plastic clay soil. The total volume of the rainfall plays a major role in the infiltration behavior for highly plastic clay soil. In addition, the successive rainfall can have a significant influence on slope failure in shallow depth in Mississippi due to several rainfall events.
- Based on the numerical analysis, it was observed that the Recycled Plastic Pin (RPP) increase the failure of safety of the slopes on Yazoo clay. The uniform spacing of RPP result in a high factor of safety and significantly less deformation near the crest of the 2H: 1V slope. On the other hand, the varied spacing of RPP (configuration D, E, and F) result in a high factor of safety. However, it has significant deformation near the crest of the slope. Thus the uniform configuration is recommended for 2H: 1V slope.
- The spacing of RPP at top section had a significant effect on the deformation of the slope for 3H: 1V and 4H: 1V slope when the failure of the slope initiates from the crest. With closer RPP spacing at the top section, the deformation of the slope is low. As a result, the effect of RPP spacing at bottom section is not significant for the performance. However, with an increase in RPP spacing at the bottom section, the factor of safety of slope decrease. The varied spacing of RPP (configuration D, E, and F) has the similar safety and performance as the uniform spacing of RPP (configuration

A, B and C). Since the varied spacing requires less number of RPPs, it will cost prohibitive and thus recommended for 3H: 1V and 4H: 1V slope.

- The current study also presents the development of a design approach for slope stabilization using RPP. The design approach was developed based on two limiting criteria which considered the horizontal displacement of RPP to ensure the performance, and maximum flexure of RPP to resist creep failure. A robust analysis was conducted, using the FEM in Plaxis, to develop the design chart for different soil strengths, slope ratios, and depths of slip surfaces. Based on the design chart, the lowest limit resistance of RPP was evaluated and grouped into four soil types based, on the lateral resistance of RPP.
- The developed design charts were utilized to determine the limit resistance of RPP and the factor of safety of reinforced slopes, using infinite slope approach. The predicted factor of safety, using the design charts which were compared with the numerical analysis results, indicated that the proposed method was in good agreement with the numerical method and can be utilized to determine the factor of safety of the reinforced slope. In addition, the infinite slope approach had the lowest factor of safety and resulted in a conservative design. Thus, the infinite slope approach is recommended, using maximum limiting horizontal displacement up to 5 cm.
- The design chart was developed for the special consideration of RPP. Therefore, the minimum length of RPP should be at least 3 m for the design. In addition, the material should be of structural grade (commercially available, with minimum flexural stress = 9.75 kPa), with the minimum cross-sectional area and moment of inertia of 79 cm^2 and 520 cm^4 respectively.

Appendix A: Sample Calculations

Sample Calculation: Infinite Slope Approach

Given:

Table A. 1 Sample Calculation Data

Slope Type	Slope Height	Slope Inclination	Top Soil			Foundation Soil		
			c	φ	ϒ	c	φ	ϒ
	m		kPa	deg	kN/m^3	kPa	deg	kN/m^3
Slope 1	12.19	3H:1V	9.57	10	19.6	19.15	30	19.6

d =2.13 m

L =38.5 m

β = 18.42˚

ϒ’ = 19.6 kN/m^3

Υ_{sat} = 19.6 kN/m^3

Factor of Safety of Unreinforced Slope:

h = d/cosβ = 2.13/cos18.42 = 2.24 m

$$FS = \frac{c' + h\,\gamma' cos^2\beta * tan\varphi'}{\gamma_{sat} * h * sin\beta * cos\beta}$$

$$FS = \frac{9.57 + 2.24 * 19.6 * cos^2 18.42 * tan10}{19.6 * 2.24 * sin18.42 * cos18.42} = 1.25$$

The factor of Safety of Reinforced Slope:

1. Selection of RPP

Based on different commercially available samples, the following RPP was selected for the design.

RPP Properties:

Dimension of RPP: 8.89 cm x 8.89 cm

Ultimate Flexural Strength: 27.57 MPa

Allowable Flexural Strength: 27.57*0.3= 8.271 MPa

2. Limit Resistance of RPP

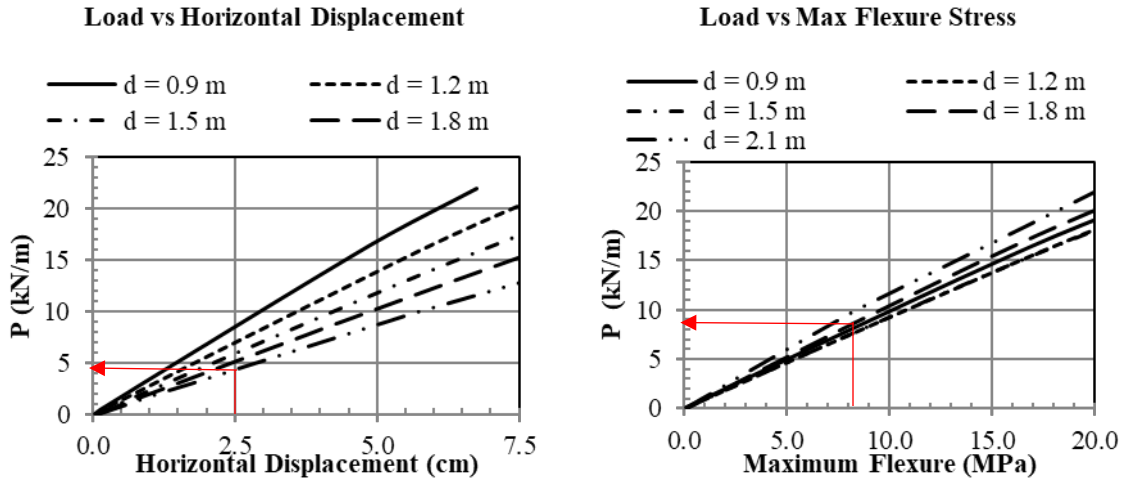

Figure A. 1 Determination of Limit Resistance of RPP

As it shown in above Table A.2, from the left plot, for 2.5 cm horizontal displacement we reached to P=4.5 kN/m, and similarly, from the right plot, for Allowable Flexural Strength P=8.271 MPa that is found in above section 1, we reached to P=8 kN/m. Therefore, the Min P=4.5 kN/m is considered.

3. Factor of Safety Calculation

P = 4.5 kN/m

S = 0.91 m c/c

$$FS = \frac{c'L + hL\,\gamma' cos^2\beta * tan\varphi' + \left(\frac{L}{s}+1\right) * P}{\gamma_{sat} * hL * sin\beta * cos\beta}$$

$$FS = \frac{9.57 * 38.5 + 2.24 * 38.5 * 19.6 * cos^2 18.42 * tan10 + \left(\frac{38.5}{0.91}+1\right) * 4.5}{19.6 * 2.24 * 38.5 * sin18.42 * cos18.42} = 1.64$$

References

- Bowders, J., Loehr, J., Salim, H., and Chen, C. (2003). "Engineering Properties of Recycled Plastic Pins for Slope Stabilization." Transportation Research Record: Journal of the Transportation Research Board.
- Breslin, V., Senturk, U., and Berndt, C. (1998). "Long-Term Engineering Properties of Recycled Plastic Lumber in Pier Construction". Resources, Conservation and Recycling.
- Bulut, R., Lytton, R. L., & Wray, W. K. (2001). "Soil suction measurements by filter paper. In Expansive clay soils and vegetative influence on shallow foundations.
- Bureau of Transporation Statistics (2015), "State Transportation Statistics 2015" , U.S. Department of Transportation.
- Chen, C. W., Salim, H., Bowders, J., Loehr, E., and Owen, J. (2007). "Creep Behavior of Recycled Plastic Lumber in Slope Stabilization Applications". *J. Mater. Civ. Eng.*
- Damiano, E., Mercogliano, P. (2013). "A simulation chain for early prediction of rainfall-induced landslides". Springer, International Publisher Science, Technology, Medicine.
- Das, B. M., 'Advanced Soil Mechanics, 3rd edition, Taylor & Francis Group, New York, 2008.
- Das, Braja M., Soil Mechanics Laboratory Manual, Oxford Press, 8th Ed. 2012.
- Day, R. W. (1996). Design and Repair for Surficial Slope Failures. Practice Periodical on Structural Design and Construction, 1(3), 83-87.
- Day, R. W., Axten, G. W. (1989). "Surficial stability of compacted clay slopes". J. Geophys. Eng.
- Douglas, S. C., and Dunlap, G. T. (2000). "Light commercial construction on Yazoo clay". Proc., 2nd Forensic Congress, ASCE, Reston, Va., 607–616.
- Elias, V., B. Christopher, and R. Berg, Mechanically Stabilized Earth Walls and Reinforced Soil Slopes Design and Construction Guidelines, Report FHWA-NHI-00-043, Federal Highway Administration, Washington, D.C., 2001.
- Fay, L., Akin, M., & Shi, X. (2012). Cost-Effective and Sustainable Road Slope Stabilization and Erosion Control (Vol. 430). Transportation Research Board.
- Genuchten, V. (1980). "A closed-formed equation for predicting the hydraulic conductivity of unsaturated soils". Soil Sci.
- Griffiths, D. V., Lane, P. A. (1999). "Slope stability analysis by finite elements. Geotechnique 49 (3).
- Hossain, J. and Hossain, M.S. (2012). "Numerical Modeling for Remedial Measures of Shallow Slope Failure Using Recycled Plastic Pins". GeoCongress 2012, ASCE, Reston, VA.
- Hossain, J., Khan, M.S., Hossain, M.S. and Ahmed, A. (2016) "Determination of Active Zone in Expansive Clay in North Texas through Field Instrumentation", *Proc. 95th Annual Meeting of Transportation Research Board*, January 10-14, 2016, Washington, DC, USA.
- Hossain, M. S., Hossain, J., Lozano, N., Khan, M.S., Kibria, G. (2012). "Investigation of geohazard potential of highway embankment slopes on expansive clay by using geophysical method". Geocongress. American Society of Civil Engineers, Oakland, CA.
- Hossain, M.S., Khan M.S. and Kibria, G. (2017), "Sustainable Slope Stabilization using Recycled Plastic Pin", CRC Press, ISBN 9781138636101 - CAT# K32128
- Hossain, S., Ahmed, S., Khan, M. S., Aramoon, A., Thian, B. (2017). "Expansive Subgrade Behavior on a State Highway in North Texas". Geotechnical and Structural Engineering Congress.
- Jiminez, M. (2004). "Assessment of Geotechnical process on the basis of sustainability principles", M. Sc. Thesis, University of Birmingham, United Kingdom.
- Johnson, L. D. (1973). "Properties of expansive clay soils, Jackson field test section study", Report 1, Misc. Paper S-73-28, U.S. Army Engineer Waterways Experiment Station, Vicksburg, Mississippi.

- Jutkofsky, W. S., Sung, J. T., & Negussey, D. (2000). Stabilization of embankment slope with geofoam. Transportation Research Record: Journal of the Transportation Research Board, 1736(1), 94-102.
- Kalinski, M., Soil Mechanics Lab Manual, 2nd edition, Wiley, 2011.
- Khan M. S., Nobahar M., Ivoke J., and Amini F. Effect of Rainfall on Slope made of Yazoo Clay soil in Mississippi. Transportation *Research Record: Journal of Transportation Research Board, 2018, (*under review).
- Khan, M. S. (2013). "Sustainable Slope Stabilization using Recycled Plastic Pin in Texas". Ph.D. Dissertation, The University of Texas at Arlington, Arlington, TX.
- Khan, M. S. and Hossain, M. S. (2015). Effect of Shrinkage and Swelling Behavior of High Plastic Clay on the Performance of a Highway Slope Reinforced with Recycled Plastic Pin. *Proc. 94th Annual Meeting of Transportation Research Board*, Washington D.C.
- Khan, M. S., Hossain, M. S., and Lozano, N. (2014). "A Numerical Study on Slope Stabilization Using Recycled Plastic Pin". Geo-Congress 2014, Geo-Characterization and Modeling for Sustainability, Reston, VA.
- Khan, M. S., Hossain, S., Ahmed, A., & Faysal, M. (2017). Investigation of a shallow slope failure on expansive clay in Texas. *Engineering Geolo*gy, 219, 118-129.
- Khan, M., Hossain, S., and Kibria, G. (2015). "Slope Stabilization Using Recycled Plastic Pins." J. Perform. Constr. Facil., 10.1061/ (ASCE) CF.1943-5509.0000809, 04015054.
- Khan, M., Kibria, G., Hossain, M., Hossain, J., and Lozano, N. (2013) Performance Evaluation of a Slope Reinforced with Recycled Plastic Pin. Geo-Congress 2013: pp. 1733-1742.
- Khan, M.S., Hossain, M.S., Ahmed, A. and Faysal, M. (2016), "Investigation of a shallow slope failure on expansive clay in Texas", Eng. Geol., http://dx.doi.org/ 0.1016/j.enggeo.2016.10.004
- Khan, M.S., Kibria, G., Hossain, M.S., Hossain, J., and Lozano, N. (2013). "Performance Evaluation of a Slope Reinforced with Recycled Plastic Pin". GSP-231, Proc. Geo-Congress, ASCE, Reston, VA.
- Kibria, G., Hossain, M., and Khan, M.S. (2013). "Influence of Soil Reinforcement on Horizontal Displacement of MSE wall." *Int. J. Geomech.*, 10.1061/ (ASCE) GM.1943-5622.0000297 (Feb. 22, 2013).
- Lampo, R. and Nosker, T. J. (1997). "Development and Testing of Plastic Lumber Materials for Construction Applications". US Army Corps of Engineers, Construction Engineering Research Laboratories, USACERL Technical Report.
- Lee Jr, L. T. (2012). "State Study 151 and 236: Yazoo Clay Investigation" (No. FHWA/MS-DOT-RD-11-236).
- Loehr, J. E. and Bowders, J. J. (2007). "Slope Stabilization using Recycled Plastic Pins – Phase III". Final Report: RI98-007D, Missouri Department of Transportation, Jefferson City, Missouri.
- Loehr, J. E., Bowders, J. J., Owen, J. W., Sommers, L., and Liew, W. Stabilization of Slopes Using Recycled Plastic Pins. Transportation Research Record: Journal of Transportation Research Board, No. 1714, Transportation Research Board of the National Academies, Washington, D.C., 2000, pp. 1-8.
- Loehr, J. E., Fennessey, T. W., & Bowders, J. J. (2007). Stabilization of surficial slides using recycled plastic reinforcement. Transportation Research Record: Transportation Research Record, 1989(1), 79-87.
- Malcolm, G. M. (1995), "Recycled Plastic Lumber and shapes design and specifications", Proc. Structures congress 13, Boston, Massachusetts, April 2-5, 1995.
- Malcolm, G. M. (1995). "Recycled Plastic Lumber and Shapes Design and Specifications". *P*roc. Structures congress 13, April 2-5, Boston, MA, 1995.
- McCormick, W., and Short, R. (2006). "Cost-effective stabilization of clay slopes and failures using plate piles." Proc., IAEG2006, Geological Society of London, London, 1–7.
- Mclaren, M. G., and Pensiero, J. P. (1999). "Simplified Design of Recycled Plastic as Structural Materials". Composites Institute's International Conference Proceedings. CRC Press LLC.

- National Oceanic and Atmospheric Administration Daily Climate Report, 2014a.
- Pearlman, S.L., B.D. Campbell, and J.L. Withiam, "Slope Stabilization Using In-Situ Earth Reinforcements," In Proceedings of the Conference on Stability and Performance of Slopes and Embankment II (GSP 31), 1992, pp. 1333–1348.
- PLAXIS 2D (2010), "Reference Manual", Version 2010.01.
- Plaxis Reference Manual: Plaxis Manual. Plaxis bv, 2011, ISBN-13:978-90-76016-22-1. www.plaxis.nl.Khan, M. S., Hossain, S., Ahmed, A., & Faysal, M. (2017). Investigation of a shallow slope failure on expansive clay in Texas. *Engineering Geolo*gy, 219, 118-129.
- Rogers, L.E. and Wright, S. G. (1986). "The effect of Wetting and Drying on the Long-Term Shear Strength Parameters for Compacted Beaumont Clay". Research Rep. 436-2F, Center for Transportation Research, the University of Texas at Austin, 1986.
- Santi, P. M., Elifrits, C. D., & Liljegren, J. A. (2001). Design and installation of horizontal wick drain for landslide stabilization. Transportation Research Record: Journal of the Transportation Research Board, 1757(1), 58-66.
- Short, R. and Collins, B.D., (2006), "Testing and Evaluation of Driven Plate Piles in Full-Size Test Slope: New Method for Stabilizing Shallow Landslides", TRB 85th Annual Meeting Compendium of Papers CD-ROM, January 22-26, Washington D.C.
- Skempton, A.W. (1977). "Slope Stability of Cuttings in Brown London Clay". In *Proceedings of Ninth International Conference on Soil Mechanics and Foundation Engineering*, Tokyo, Vol. 3, 261-270.
- Stephens, I., & Branch, A (2013). "Testing Procedure for Estimating Fully Softened Shear Strengths of Soils Using Reconstituted Material (No. ERDC/GSL-GEOTACS-TN-13-1). Engineering Research and Development Center Vicksburg MS Geotechnical and Structural LAB.
- Taquinio, F. and Pearlman, S.L. (1999). "Pin Piles for Building Foundations," presented at the 7th Annual Great Lakes Geotechnical and Geoenvironmental Conference, Kent, Ohio, May 10.
- Taylor, A.C. (2005). "Mineralogy and engineering properties of the Yazoo clay formation", Jackson Group, Master's Thesis, Mississippi State University.
- Titi, H., Helwany, S., 2007. Investigation of vertical members to resist surficial slope instabilities, (WHRP 07–03). Wisconsin Department of Transportation, Madison, WI.
- Tohari, A., Nishigaki, M., and Komatsu, M. (2007). "Laboratory rainfall induced slope failure with moisture content measurement". J. Geotech. Geoenviron., 133, 575–587.
- Turner, A. K., and Schuster, R. L., 1996. Landslides— Investigation and mitigation: National Research Council, Transportation Research Board Special Report 247, National Academy Press, Washington, D.C.
- US Army Corps of Engineers (USACE). 1970. *Laboratory soils manual*. EM 1110-2-1906. Vicksburg, MS:US Army Corps of Engineers Waterways Experiment Station.
- Wright, S. G. (2005). "Evaluation of Soil Shear Strengths for Slope and Retaining Wall Stability Analyses with Emphasis on High Plasticity Clays." FHWA/TX-06/5-1874-01-1, Federal Highway Administration, Washington, D.C.